2017-01-01

Comparison Of Extruder Systems For 3d Printer Filament Fabrication

Adriana Ramirez
University of Texas at El Paso, aramirez53@miners.utep.edu

COMPARISON OF EXTRUDER SYSTEMS FOR 3D PRINTER FILAMENT FABRICATION

ADRIANA RAMIREZ

Master's Program in Metallurgical and Materials Engineering

APPROVED:

David A. Roberson, Ph.D., Chair

Stephen Stafford, Ph.D.

Mahesh Narayan, Ph.D.

Charles Ambler, Ph.D.
Dean of the Graduate School

Dedication

To God,

My parents,

Francisco and Sandra Ramirez

Siblings,

Andrea, Francisco and Roberto

And

My little Luna

Who have been with me through this journey,

their unconditional love and support has given me the strength

to achieve my academic and life goals.

COMPARISON OF EXTRUDER SYSTEMS FOR 3D PRINTER FILAMENT FABRICATION

by

ADRIANA RAMIREZ

CHEMISTRY BS

THESIS

Presented to the Faculty of the Graduate School of

The University of Texas at El Paso

in Partial Fulfillment

of the Requirements

for the Degree of

MASTER OF SCIENCE

Metallurgical, Materials and Biomedical Engineering

THE UNIVERSITY OF TEXAS AT EL PASO

May 2017

Acknowledgements

Coming from another department has been one of the biggest challenges throughout my academic path; I would like to offer my appreciation to all the people that made this possible. I would like to express my deepest gratitude to my advisor, Dr. David A. Roberson for giving me the opportunity to work in his Polymer Extrusion Lab during the last two years. Thank you, Dr. Roberson for introducing me to the department, I would always be grateful for your guidance, patience, and support. In addition, I am indebted to all of the MMBE department professors, for their time and availability, to answer my questions pertaining their classes. Thank you to the W.M. Keck center 3D innovation, for allowing me to be part of one of their laboratories, as well as for allowing me to use their equipment for my projects. My sincere thanks to Dr. Stafford and Dr. Narayan, for been part of my committee, and for always providing academic support.

Thank you to Brenda Torres and Maryam Zarei for encouraging me to pursue a higher academic degree especially in the field of Materials Science Engineering; for their guidance and friendship. To the members of the polymer extrusion lab: Carmen Rocha, Kevin Schnittker, Francisco Andrade, Gilberto Siqueiros, Truman Word, and Victor Vargas for their encouragement and collaboration during these two years. To my classmates who were always there for me: Lupita Huerta, Ana Rios, Ale Melendez, Israel Martinez, Jorge Catalan, and Shusil Bhusal, their friendship will nourished forever. To my friend Summer Gonzalez, who stayed up with me every night at UTEP while I worked on my thesis. To Mr. and Mrs. Chan for all of their help and guidance in my academic career. Last but not least my eternal gratitude to my Family, for all their support, patience, and motivation; they are the shoulders on which I stand.

Abstract

Additive Manufacturing (AM) has grown in popularity over the past thirty years, due to its versatility, short design to product cycle, and capability to fabricate complex geometries, which cannot otherwise be produced. There exist several platforms that are able to print objects composed of different materials, making this technology significant in different fields such as: automotive, aerospace, medical, electronics, amongst others. Though several types of AM technologies are available, the expiration of the patents on fused deposition modeling (FDM) in 2009 has led to a widespread use of this platform in academia and home use settings.

Widespread use of FDM-type AM platforms has led to a demand to fabricate feedstock materials for this AM platform. Particularly, in the home do it yourself (DIY) community there has been a widespread interest for users to manufacture their own feedstock filament leading to a large growth in home-use extrusion systems. The low cost of these desktop-grade systems has also made them attractive to academics, but there has not been a widespread effort into determining the efficacy of these small scale extrusion systems as compared to industrial quality extruders which are typically used to manufacture feedstock for FDM platforms.

The aim of this study was to compare two extrusion processes: 1) a desktop grade single-screw extruder; and 2) an industrial scale twin-screw extruder. In order to understand differences between their performance and quality of mixing, a rubberized blend of acrylonitrile butadiene styrene (ABS) mixed with styrene ethylene butylene styrene with a maleic anhydride graft (SEBS-g-MA) at different ratios was compounded on each extrusion system. Melt flow index, and mechanical properties were compared. In addition, a raster pattern sensitivity study was performed to evaluate the effect of the extruder system on 3D printed objects. Finally, scanning electron microscopy (SEM) was used to examine the fracture surfaces of spent tensile specimens.

Table of Contents

List of Tables

List of Figures

Chapter 1: Statement of Purpose

Additive Manufacturing (AM), also known as 3D printing was developed by the physicist Charles Hull in 1986 after developing stereolithography, which involves photocurable resins. In addition to Hull's work, a fused deposition modeling (FDM) patent by Scott Crump in the 1990s increased research investigations pertaining to 3D printing [1], [2]. AM technologies that involve layer-by-layer manufacturing such the case of Fused Deposition Modeling, have become very competitive because of the high demand in materials. These materials must be improved in both its quality and performance in comparison to its conventional standards, which include AM systems that are developed from a single material [3]. Due to high demand in materials, advances of Multiple Material Additive Manufacturing (MMAM) had been introduced, promising a better performance by providing the opportunity to use a multiple material system. MMAM systems offer strategies that improve mechanical properties, additional functionality and design freedom to meet currently product demands [4].

According to literature published in March 2012, president Obama announced The National Network for Manufacturing Innovation (NNMI). This brought an increase in the U.S. manufacturing competitiveness, triggering federal agencies, universities, community colleges and state governments to invest in industrial manufacturing technologies with a wide range of applications. NNMI allowed the research expansion of additive manufacturing not only because of its applications, but mostly for its economical and sustainability viewpoint. In general, NNMI has made improvements with respect to material waste reduction, energy consumption, time efficiency production, and fabrication of complex parts; making these characteristics a bigger advantage compared to those provided by the use of traditional manufacturing techniques [5].

Research in additive manufacturing, has grown mostly in academia. Now a days it is easier to acquire a personal desktop AM machine at a low cost, enabling researchers to learn more about this technology by putting hands-on work. The research with respect to the improvement and development of suitable materials is necessary and currently in process by many researchers. As it was previously mentioned the use of Multiple Material Additive Manufacturing plays an important role in the field. There are many research studies where material properties are intended to be improved by the incorporation of one or more materials. In the particular case of polymers, there are different investigations where mechanical properties are being improved by the addition of fillers in the polymeric matrix [6],[7].

In general, these investigations involve the use of the extrusion process for the production of polymeric monofilaments used for 3D printing [8]. Extrusion process can vary depending on the application, for this particular technology, there are two types of extrusion systems: 1) single-screw extruder and 2) twin-screw extruder. One of the advantage to own a personal extruder is that less materials are wasted and enables the researcher create a multiple material for 3D printing.

Investigations on behalf the improvement of properties in polymeric monofilaments has increased, however there is a lack of research on the selection of equipment to produce polymeric monofilaments for 3D printing. As mentioned earlier both systems of extrusion can be used for the production of polymeric filaments, bringing the question which one of those will be a better performer or which one can the researcher rely on. It can be hypothesized that the twin-screw extruder could be more effective, due to the mechanical complexity that the system owns compared to the single screw extruder. However, what if the final product does not make that much of difference using the single screw extruder? This could be significant with respect to savings.

The aim of this investigation is to provide a stand point-of-view of the equipment selection for mixing and compounding polymeric filaments for 3D printing. Five rubberized blends with different ratios, were extruded by two extrusion systems: 1) single-screw extruder and 2) twin-screw extruder. The compounding performance of these extrusion systems was evaluated by different tests including: mechanical testing, rheological test, filament tolerances and fracture surface analysis. Finally, the use of fused deposition modeling was done to print tensile specimens with different raster angles: 0°, 45° and 90°. The purpose of using three raster angles was to analyze and compare the fracture modes generated at the surface during the tensile test.

Chapter 2: Background

2.1 Extrusion Background

The extrusion process was introduced at the end of the eighteenth century by Joseph Brama, who made a huge contribution in the manufacturing of lead pipes. Brama's creation gave rise to hot-melt extrusion in plastic industries in the mid-ninetieth century; it was first used in wire insulation polymer coating process. [9]. In the early 1930s Hot-melt extrusion (HME) became a very popular and efficient technology not only in plastic industries, but in food processing, and medical industry; to date this technique is used for the production of plastic products such as: bags, sheets, pipes, drug delivery and many more.

Hot-melt extrusion mainly involves the use of an extruder, which is composed of a feeding hopper, barrels, a single or twin screws, and a die. The main function of an extruder is to create and improve the homogeneity and compounding of a polymeric material. Finding the right parameters such as: temperature, pressure, and velocity is important for a successful outcome [10]. Generally, all the extruders count with a screw(s) situated inside the barrel, at the end of this barrel a die is found, this one can vary in size depending on the desired shape and size of the extruded product.

The screw is the fundamental component of the extruder, the rest of the components (motor, gear-box, hopper, barrel and die) are only necessary supports that empowers the proper performance of the screw [11]. In addition, extruders have an auxiliary equipment that consists of either a heating or cooling device for the barrels, a conveyer belt to cool down the product, and a water pump. There exists two classes of extruders: single-screw and twin-screw extruders, they both have their differences as shown in Figure 2.1, which will be explained in detail later in the chapter. Extruders have evolved through the years, becoming more sophisticated and suitable in manufacturing offering promising functions for a significant variety of applications [9], [10], [12].

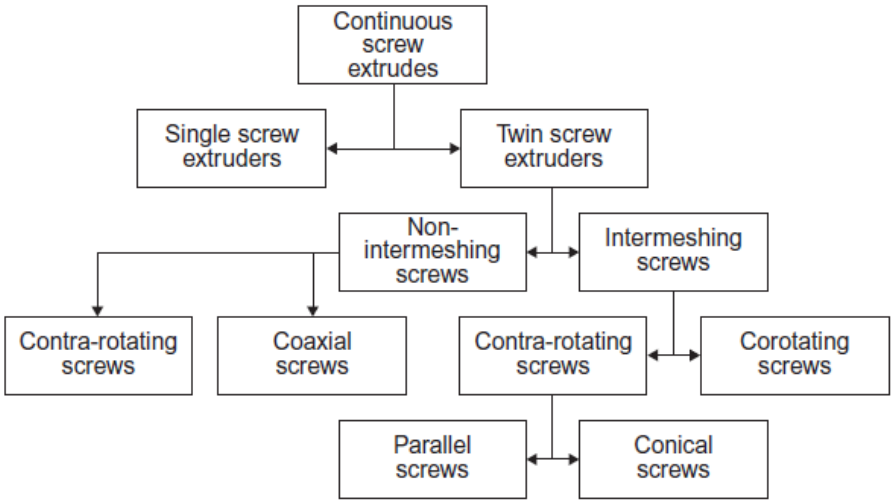

Figure 2.1.- Two classes of extruders [12].

2.2 Single-screw Extruder

A single screw extruder has been the most common and primary process of extrusion for many years even up to this date. This process counts with a simple equipment that is available at low costs in marketing [13]. It counts with a single screw in the system, in charge of three basic functions: solid conveying, melting and metering or pumping [4, 5]. These functions are conceivable by the five major equipment components that the single screw extruder possess (Figure 2.2) [14].

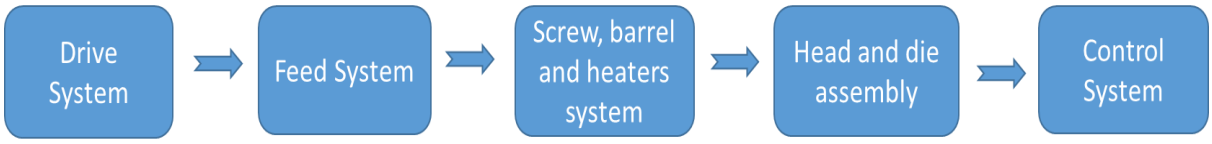

Figure 2.2.- Five major equipment components on a single screw extruder

On the other hand, Figure 2.3 illustrates the schematic of a single screw extruder. Polymer extrusion begins by feeding the material in pellet form through a hopper. A constant feeding rate is important for an effective extrusion process. The feeding rate is dependent on the characteristics and properties of the polymer. In order to have a successful feeding in the machine, there are different parameters to take into account: small pellet size, high bulk density, low internal friction between pellets, low external friction on the hopper surface, and high melting point.

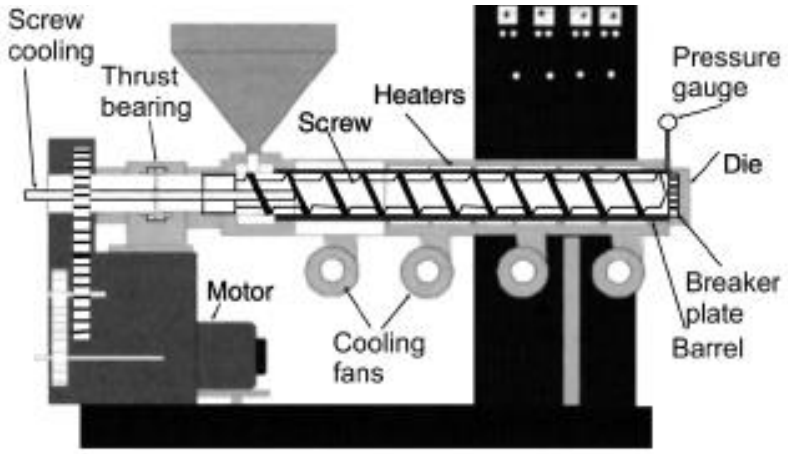

Figure 2.3.- Schematic of a single screw extruder [14].

Furthermore, once that the polymer pellets are fed they are able to get to the screw by gravitational force. The material then advances along the barrel filling up the screw, Figure 2.4 represents this feature. The material tends to rotate within the screw rotation, traveling to the heater zone, little by little the material will melt and compact. Figure 2.5 shows a representation on a fully compacted solid bed in screw feed section.

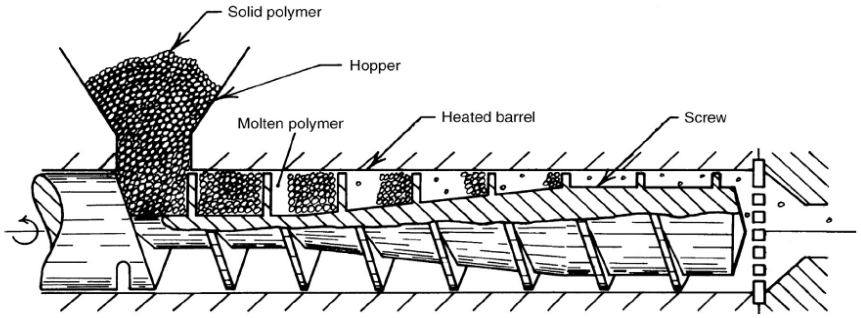

Figure 2.4.- Extrusion feeding and compacting the material [13].

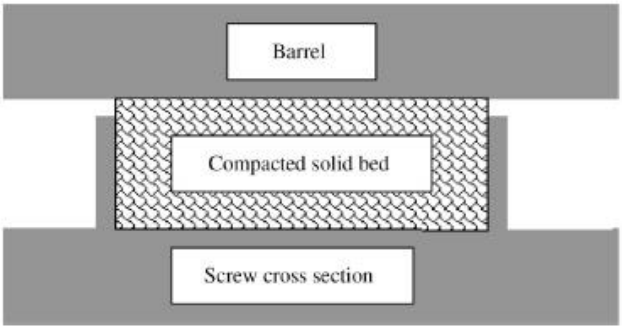

Figure 2.5.- Representation of fully compacted solid bed in screw feed section [13]

Pressure is generated due to forwarding force that is being accumulated along the screw, this one then conveys the material and forces it to exit trough the die, which is located at the end of the extruder. In order to acquire a high conveying rate during the extrusion process, a large screw channel area is preferred, as well as the use of polymers containing high viscosity, a barrel with a temperature close to the melting point of the polymer, and ideally, a screw with a temperature higher than the melting point of the polymer [11].

Normally, the material exiting the extruder varies depending on the shape and size of the die. Single-screw extruder counts with a control system, this one allows users to manipulate temperatures and the screw speed depending on the material that is been extruded. Single-screw extruders can vary depending on the screw, barrel diameter or the length to the diameter; it could be represented in the ratio form: L/D. Diameters vary from sizes ranging from 0.5mm to3.5mm. The extrusion rate capacity varies with the respective L/D, there exist extruders with short and long L/D which have their particular advantages. The advantages of extruders that count with a short and long L/D are compared in Table 2.1 [14].

Table 2.1. Advantages of short and long L/D from single screw extruder

Short L/D	**Long L/D**
Occupy small floor space	Occupy greater floor space
Replacement of parts as well and cost of the extruder is low	Greater mixing capability
Low horsepower and small motor size	Greater melting capacity
Small torque required	Higher material throughput

2.3 Twin-screw Extruder

Twin- screw extrusion has played an important role in manufacturing, especially for mixing and compounding diverse materials according to their respective applications [12]. One factor that differs a single-screw extruder from a twin-screw extruder is the amount of screws in the barrel, the process is mostly identical. This section will describe in detail the parts, components, and the process of this extrusion system. There is a wide open variety of twin-screw extruders in marketing, selection of the proper twin-screw extruder is subjected to the desired application.

However, the major difference in twin screw extruder models, vary contingent to the sort of the parallel screw shafts that the extruder possesses. There are two categories: parallel intermeshing and non-intermeshing twin screw extruders, which are dependent on the rotation on the screws. The screws can either rotate in the same direction (co-rotating) or rotate in the opposite direction (counter-rotating), Figure 2.6 represents the co-rotating and counter-rotating intermeshing screws.

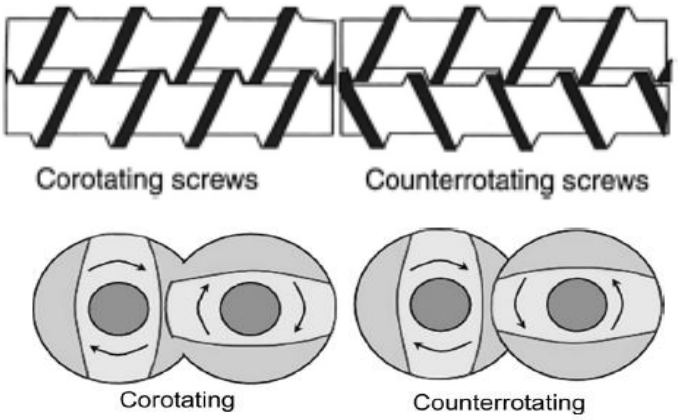

Figure 2.6.- Co-rotating and counter-rotating intermeshing screws [15]

In addition, parallel intermeshing and non-intermeshing twin-screw extruder, are dependent on the distances between screw shafts. For instance, if the centerline distance in between the shafts is less than the screw diameter the screws are known as intermeshing, whereas if the distance is equal to the screw diameter they are known as non-intermeshing [15], Table 2.2 represents a comparison of parallel twin-screw extruders and their respective properties.

Table 2.2. Comparison of parallel twin-screws in the extrusion system [15]

	Corotating Intermeshing	Counterrotating Intermeshing	Counterrotating Non-intermeshing
Practical residence time, min	0.35–6	0.35–6	0.35–6
Residence time distribution	Variable	Variable/Tighter	Variable
Dispersion	High	High	Good
Heat transfer	Excellent	Excellent	Excellent
Venting	Excellent	Excellent	Excellent
Pumping	Good	Excellent	Fair
Self-wiping	Excellent	Good	Fair
Zoning	Excellent	Excellent	Good
Output rate	High	Moderate	High
Distributive mixing	Good	Good	Excellent

The design and components of the extruder, are divided into three sections: drive, process and control section, which holds five major components of the extruder. These five major components are identical to single-screw extruder (Figure 2.7) [12].

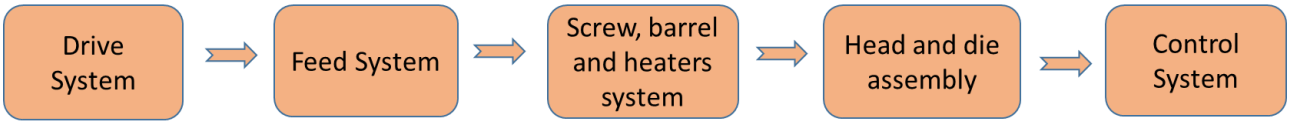

Figure 2.7.- Five major components of a twin screw extruder

The process is very similar to the single-screw extruder system, it begins by feeding the material trough the hopper and conveying it through the barrel. While the material is advancing trough the screws it mixes and melts. Usually, twin screw extruders count with different heating zones that can be manipulated by the controller system as well as the pressures, and velocities of the screws, Figure 2.8 shows a representation of a twin screw extruder.

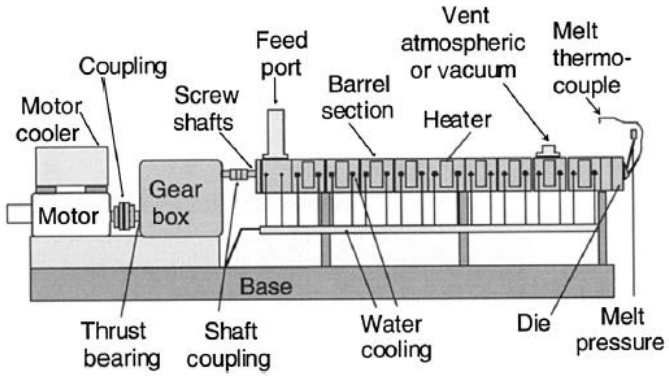

Figure 2.8.- Components for a twin-screw extruder [15]

2.4 Behavior of Plastics During Extrusion

The purpose in every thermoplastic extrusion process is to acquire a homogeneous polymer product, in order to do so there are conditions that need to be addressed in areas such as: the feed rate, melt, and mixing [16]. For instance, the feed zone experiences frictional properties that affect the efficiency of the extruder. There are two frictions that are present on the feeding section: 1) an internal friction between the individual polymer particles and formulation ingredients; 2) an external friction between the formulation components and the metal surfaces of the feed throat, barrel walls and screw root [17]. These two frictions are essential for a good material feed, the question now is how low or how high both frictions need to be? According to literature, a low internal friction allows formulation ingredients to flow freely into the extruder [16]. On the other hand, a low external friction enables the material to flow freely along the hopper walls into the extruder.

Furthermore, it is desired that the polymer progressively moves forward to the transient section. This can be achieved by having a high external friction between the selected material and the barrel, because that high friction will allow the material to stick to the barrel wall and move forward. On the other hand, another parameter to consider to aid the material to move forward, is

temperature zone 1. This one generates internal friction which allows the polymer to advance along the rotation of the screw, taking the material to the transient section [17]. As mentioned earlier, when the polymer passes the feeding zone, it begins to melt and mix reaching a homogeneous state. The barrel and the viscous shear heating, are two sources that generate heat during the process enabling the compounding of the material.

Shearing in the extruder can be generated by the movement relative to the layers within the polymer along with the movement of the plastic in parallel direction to the barrel wall or the screw. It is important to remark that function of shear is proportional to that of the screw speed. For instance, if the screw speed is increased the shear rate will rise, decreasing the viscosity of the polymer and affecting the flow of the process. Viscous heat generation in the process is the most significant factor that allows a polymer to melt in the process, due to the viscosity relative to the high shear rates from the extruder [17].

During the conveying zone, the barrel practically rotates while the plastic flows reaching the railing flight and turning upward towards the barrel surface; the process is repeated until it reaches the following pushing flight. This particular scenario is in charge to shear and mix the plastic in the metering zone. Finally, the shape of the extruded product is controlled by the die, which can be found in many sizes and shapes for polymer extrusion.

2.5 Extrusion of Polymeric Monofilaments for 3D Printing

Extrusion is a very effective process in the production of diverse kinds of monofilaments, for distinct applications. Monofilaments fiber based on polymers are commonly used for making racquetball rackets, fishing lines, strings for tennis, 3D and many more [18]. In the area of 3D printing polymeric monofilaments are essential. The extrusion of polymeric monofilaments encounters many challenges, especially for the improvement of properties achieved by the addition

of reinforcements such as: fillers or plasticizers. During this section different challenges in the extrusion of polymeric monofilaments will be discussed as well as different variables to take into account during the process.

Challenges during the extrusion of polymeric monofilaments begins by the selection of the material. Glass transition temperature is significant for the appropriate selection of extrusion temperatures during the process. Recalling section 2.4 from this chapter, viscosity of the material is dependent on the temperature, which generates the flow required to drag the material trough the barrel. Thus, temperature plays an important role during the process of extrusion. Another important factor to take into account in the case of the addition of fillers, is the compatibility of the filler with the polymer resin and how this one reacts in high temperatures environments.

In addition, a cooling source is needed after the filament exits the die. A good example is a water bath, which should be clean to avoid any cross contamination in the system. This part of the extrusion is another challenge that is faced and care is required for good quality of the filament. Not having the adequate cooling source can lead to voids inside the filament as well as an oval filament shape. This can cause an inconsistent filament diameter, which can generate printing defects. Finally, monitoring the diameter from the filament is important because this one will feed the 3D printer. The diameter can be altered by the use of a spooler that works under certain speed, which can be adjusted for the desired diameter size.

Chapter 3: Fused Deposition Modeling

3.1 Background

Fused Deposition Modeling (FDM) was developed in the late 1990s by Stratasys, Inc.,USA; it is one of the most common additive manufacturing technologies used for a diverse engineering applications. It possesses the ability to elaborate complex parts at a very efficient time and lower costs compared to conventional manufacturing processes, due to the manufacturing of a 3D-mensional object layer-by-layer [19]. One of the characteristics of FDM is that it presents properties with greater anisotropy compared to other forms of additive manufacturing. In other words, the build direction has an effect in strength and toughness resulting from the interlayer bonding in the 3D object [20]. The simplicity of usage and economical costs from this technology allow users interested in the scope of 3D printing to own a desktop-sized machine at home.

Furthermore, FDM printers are limited to thermoplastic polymers with a suitable melt viscosity. Based on research, in order to have the appropriate structural support, viscosity must be high and low enough to allow extrusion. Amongst the extended list of materials that FDM is suitable for, one can consider the use of popular materials such as: Acrylonitrile Butadiene Styrene (ABS), Styrene Ethylene Butadiene Styrene (SEBS), Polycarbonate or Polylactic acid (PLA). One of the many advantages from FDM printers is the ability to enhance deposition of distinct materials at the same time. This can be achieved by setting multiple extrusion nozzles into the printer so two materials can be loaded and extruded [21].

FDM has become useful in fields such as: aerospace, architecture, education and medical where 3D printing of polymers has become useful [22], [23]. Due to the efficiency in production of fused deposition modeling, product demands have increased, having a high quality standards of production. Therefore manufacturers must meet costumers needs, which leads to taking proper

selection of materials and parameters to improve the quality of the product [24]. The process of this technology consists on (Figure 3.1):

- Conceptualization and Computer-Aided Design (CAD)
- Conversion to STL, transfer and manipulate STL file on the 3D printer,
- Machine setup
- Build
- Part removal
- Post processing and application [25]

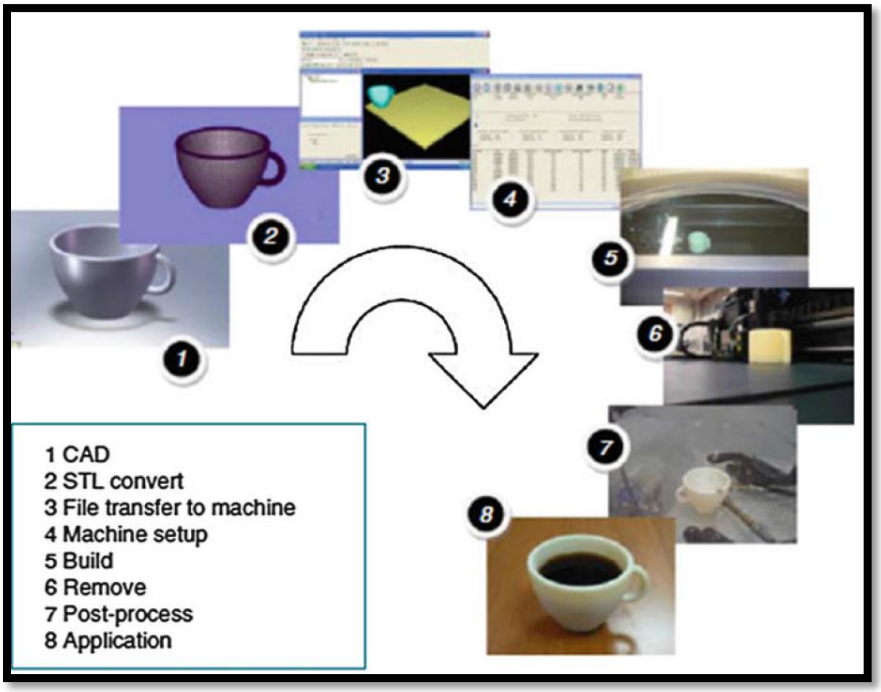

Figure 3.1.- Process of Fused Deposition Modeling [25]

3.2 Process of FDM

3.2.1 CAD to STL File

Fused deposition modeling relies on the use of a 3D modeling computer aided system design (CAD). The main purpose of the CAD software is to generate the 3D design in detail with precise measurements. 3D systems originated the Standard Tessellation Language file (STL), allowing the configuration of the three dimensional orientation between slices, printing speeds, infill percentage, size correction, position and orientation of building (Figure 3.2). The CAD design is converted to a STL file by most commercially available drafting software packages [26]. Figure 3.2 illustrates the CAD model converted to STL format.

Figure 3.2.- CAD model converted into STL format [26]

Once all the desired settings are saved, the STL file is converted into a G-code by a selected program. The G-code then follows all the settings to create a 3D object in a layer-by-layer manner. The printer can be manually adjusted with respect to nozzle temperature, printing speeds and flow, which can vary depending on the chosen material.

3.2.2 Machine set up

Melt extrusion using FDM technology is represented in Figure 3.4. A typical FDM set up consists of a machine that contains two rollers, which feed the filament down to the nozzle tip located at the end of the printer head. A key component of the melt extrusion process is the heating element that will melt the thermoplastic, this aids the material to reach the nozzle. Thus, the material begins to be deposited on a bed platform. The head of the printer moves in the horizontal X-Y plane then in the Z direction layer by layer, the process repeats until a 3D object is produced [27]. A good analogy of the FDM printing process is that of a hot glue gun. Even though FDM is a simple technique there are different issues that are present during the process. For example, the presence of surface defects that can be caused from the nature of the slicing software and the STL file format. On the other hand, internal defects can be present as well, resulting from heterogeneities in the filament diameter affecting the way the material is extruded from the printer nozzle [28].

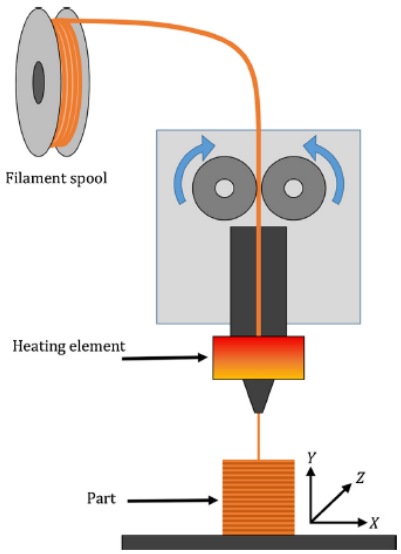

Figure 3.4.- Machine set up for a FDM technology [20]

3.3 Printing Parameters

One of the challenges that are present 3D printing is finding the adequate printing parameters with respect to the material that is being used and the design one intends to print. This section will discuss optimal parameters to take into account to obtain a successful print.

- **Nozzle and bed platform temperatures:** The adequate temperatures from the heating elements in the head of the printer, will be in charge to melt the filament that is been feed by the system. On the other hand, the bed or platform where the material is deposited requires an appropriate temperature to aid the first layer of the print to stick into the bed platform settling it in a stationary position, to start building the object in a layer-by-layer manner. Inner stresses, and interlayer deformation are caused during the process when printing, due to the melting and solidification at the environment temperature. Weak bonding can arise if changes of temperatures in the system are not monitored or controlled, leading to warping, distortions or even complete failure to print the object [29].

- **Flow:** The flow refers to the percentage of material that is deposited in the bed platform. This parameter can be manipulated since it is dependent on the filament diameter, the diameters can vary depending on the 3D printer model; the diameter size most commonly used are 1.75mm or 3.00mm. If the diameter is smaller of what it is supposed to be the flow can be increased in order to prevent any voids or air gaps in the printed object. However, this is not the case where the filament is greater of what it supposed to be. If the filament is too large, clogging can occur, affecting quality of the printing or failure to print the part.

- **Layer thickness:** Refers to the thickness of the layer that is deposited by the nozzle tip (Fig 3.5). This parameter is dependent on the nozzle tip size, which can range from 0.4mm to 0.8mm. The layer thickness influences the mechanical properties of the 3D object. The bottom surface tends to accumulate residual stresses during fabrication causing distortions. Therefore, the deformation in the bottom layer tends to be greater than the top layer [30].

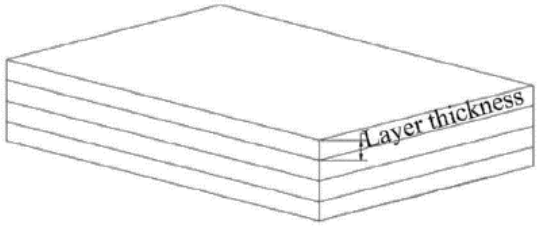

Figure 3.5.- Layer thickness[24]

- **Printing speeds:** This variable helps in cases where 3D objects are printed by the use of complex materials. The printing speed prevents printing defects such as delamination or an uneven deposition [30]. For instance, there are cases where the speed is too fast, that the counter perimeter or even the infill is not able to stick into the previous printed layer, causing air gaps in between layers. The right selection of printing speed not only prevents defects in the object, but can also help to fabricate an object at an efficient time when no problems with the material are present.

- **Build orientation:** The build orientation is defined as the inclination of part in a build platform with respect to XYZ axis. According to literature research, this parameter aligns polymer molecules along with the direction of deposition when the object is been fabricated [31]. Anisotropic properties arise depending on the building orientation, making this

parameter one of the most important since it determines mechanical properties and build time, rather than dimensional accuracy or surface roughness [32].

- **Raster angle:** is referred as the distance between two adjacent deposited filaments within the same layer. The most common raster angles that are used for 3D printing are 0°, 45° and 90°. Raster angle is another parameter where mechanical properties can be affected depending on the raster angle used (Fig. 3.6).

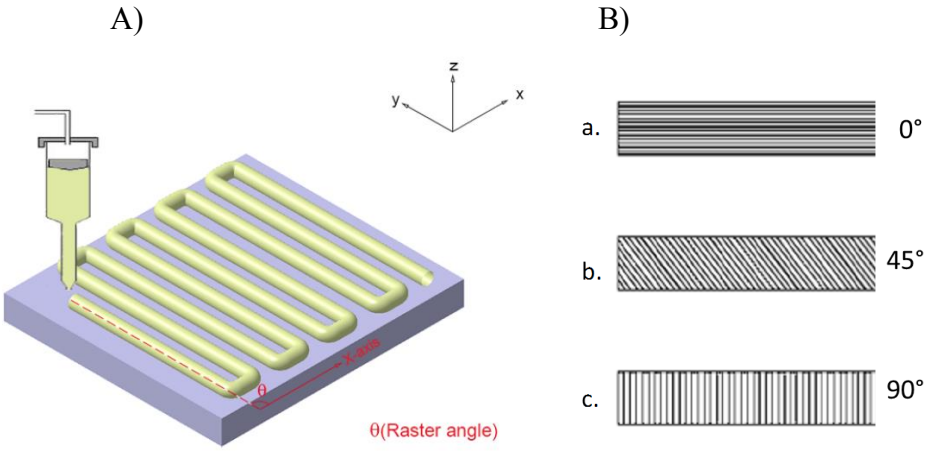

Figure 3.6.- (A) Raster angle in XYZ direction. From [33] (B)Different Raster angles used in 3D printing. From [34].

- **Infill pattern:** is defined as the pattern of the material that is internally located in the object. There are standard types of patterns such as honeycomb, rectilinear or triangular. Infill pattern is considered to be another fundamental parameter for 3D printing. The parameter can compromise different advantages regarding mechanical properties, material or filament conservation, lightening of the object and the improvements of the internal structure [35]. The different infill pattern that can be used for printing are illustrated in Figure 3.7.

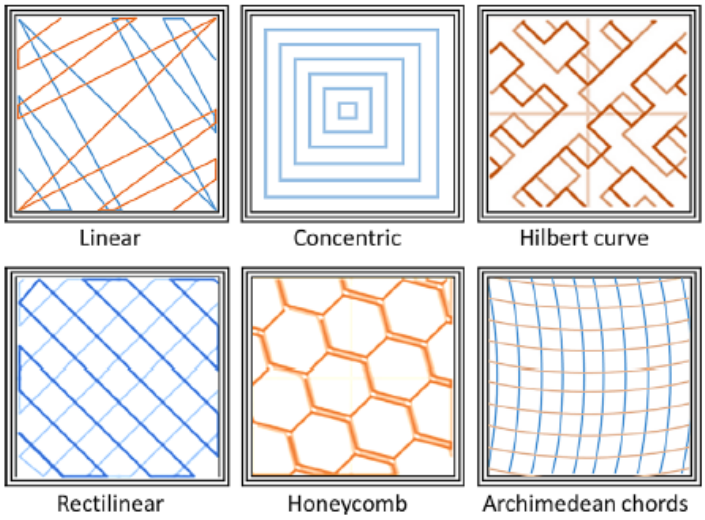

Figure 3.7.- Different Infill patterns used for 3D printing. From[35]

- **Air gaps:** are referred to the space between the beads that are deposited by the nozzle in the process of printing. In addition, it is a process parameter that can affect tensile strength along with raster orientation compared to the rest of the printing parameters [36]. There are two types of air gaps: 1) a positive air gap, indicates that two adjacent roads from the layer do not touch; 2) a negative air gaps, reduce void fraction present between roads a increases bond area, however, it tends to cause distortion in the dimension of the object (Figure 3.8) [37].

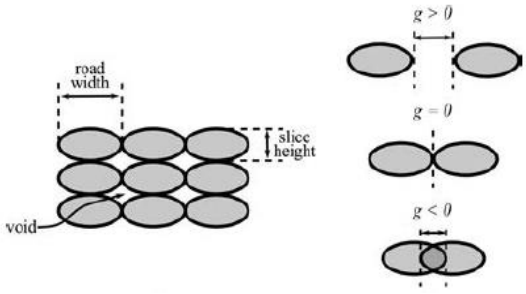

Figure 3.8.- Different Air gaps that can be present in 3D printing. From [37]

3.4 Polymers

Humans have used polymers for thousands of years. Polymers are characterized as long molecules that are covalently bonded backbone of carbon atoms. Polymers can be found in almost all biological systems such as wood, bone, cartilage, or leather. They have the ability to regulate chemical reactions in living organisms like cells or veins. Microstructure of polymers is much more complex than those observed in metals and ceramics. However, the manufacturing through the use of polymers is not that difficult and they are considered to be inexpensive for distinct applications [38]. During the last century, researchers have synthesized a wide variety of polymers with a broad range of mechanical properties. Is has long been known that most polymers do not possess the mechanical properties that metals and ceramics have. Because of this fact, scientists have developed research to improve polymer properties through the creation of composites and other means. Industries in particular have been able to work in the production of reinforced polymers, making improvements that have shown a great impact on polymer properties such as stiffness, strength among others [39].

Polymer reinforcements have become popular in a wide range of applications such as sports, medical, and aerospace. Recent investigations have reported results where the mechanical properties of polymers have improved, that they can now possess properties similar to metals like aluminum. Hence, properties in polymers should be well studied and understood because they can change by the addition of one or more components.

Polymers are divided into three classes:

-Thermoplastics

-Thermosets/Resins

-Elastomers

3.4.1 Thermoplastics

Based on literature, the prominent characteristic from thermoplastics is that they are linear polymers that are easily softened when heat is applied. This class of polymers can have different configurations, which means that they can be in a crystalline or amorphous form. The structure of this class depends on long chains formed by the addition of sub-units best known as "monomers," in a repeated sequence. Common thermoplastics: polyethylene (PE), polypropylene (PP), polytetrafluoroethylene (PTFE), polystyrene (PS), polyvinylchloride (PVC), amongst others [40].

3.4.2 Thermosets

Thermosets are classified as network polymers, meaning that they are heavily cross-linked. The polymerization consists of the combination of a resin and a hardener, these two react and harden. The structure is always amorphous due to the cross-linking during polymerization. Cross-linking plays an important role for thermosets, they are not able to melt when heat is added. If the polymer is exposed to a high temperature it can cause decomposition. Thermosets are good for purposes such as polymer reinforcements, molding and hard surfacing or electrical fittings. Common thermosets used are: epoxy, polyester, and phenol-formaldehyde.

3.4.3 Elastomers

Elastomers are also known as rubbers they are usually linear polymers. However, there are cases where cross-links are present in the structure. The property that arises in the presence of cross-links is the recovery of the material to its original place [41].

3.4.4 Mechanical Behavior of polymers

There are different mechanisms that polymers can pass through, starting from brittle–elastic at low temperatures, then to a rubbery stage and finally, to a viscous state at high temperatures. The mechanical state of the polymer is based on the molecular weight and how close the temperature is to its glass transition temperature (T_g). At room temperature the polymer is in a rigid form, when heat is added, molecules tend to gain energy allowing the movement of molecules around. Therefore, glass transition temperature (T_g) can be defined as the temperature required to give freedom of mobility to molecules in a polymer been in a rigid state [39]. In order to understand the mechanical behavior of plastics, the difference between stiffness and strength of polymers should be understood. The stiffness is the resistance to elastic deformation, and strength is the resistance to collapse by plastic yielding or by fracture. There are five deformation stages of polymers shown in Figure 3.9 [39] :

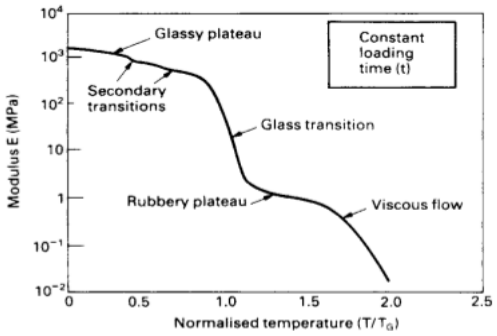

Figure. 3.9.- Five deformation stages of polymers. From [39]

-Glassy stage: In this phase of the system the polymer is below T_g where molecules are packed, tightly together and in an amorphous form. Adding load causes stretching in the bonds, leading to elastic deformation. Modulus in polymers can be increased by the orientation of molecules of the polymer

-Glass transition stage: During this state the temperature starts to increase causing secondary bonds to break, additionally there is a decrease in modulus.

-Rubbery stage: In this stage the modulus is small, approximately one thousandth of the glassy modulus. Having frequent cross-links can affect this stage; covalent bonds form three-dimensional networks, affecting the melting of secondary bonds in the polymer.

-Viscous stage: During this stage, bonds are completely melted and polymer begins to flow. In the case of thermoplastics due to the linear structure that they possess, the polymer has the tendency to become viscous liquid.

-Decomposition stage: in this phase the polymer gets to a very high temperature causing the degradation of the polymer.

Chapter 4: Experimental Procedure

In general, the experimental procedure for this study was based on the extrusion of five polymeric blends that varied in percentage by weight. These five polymeric blends were processed by two extrusion systems: 1) single-screw extruder and 2) twin-screw extruder. Once the polymeric blends from each extrusion system were obtained, tensile specimens were printed with three raster orientations, by the use of fused deposition modeling. Mechanical testing was performed on tensile specimens, and fracture surface analysis from the breakage part of the specimen was analyzed by a scanning electron microscope. In addition, rheological tests was achieved by each of the polymeric blends extruded. Finally, filament tolerances were obtained by measuring the diameters and compare the consistency in size. During this chapter, the experimental procedure will be explained in detail as shown in figure 4.1.

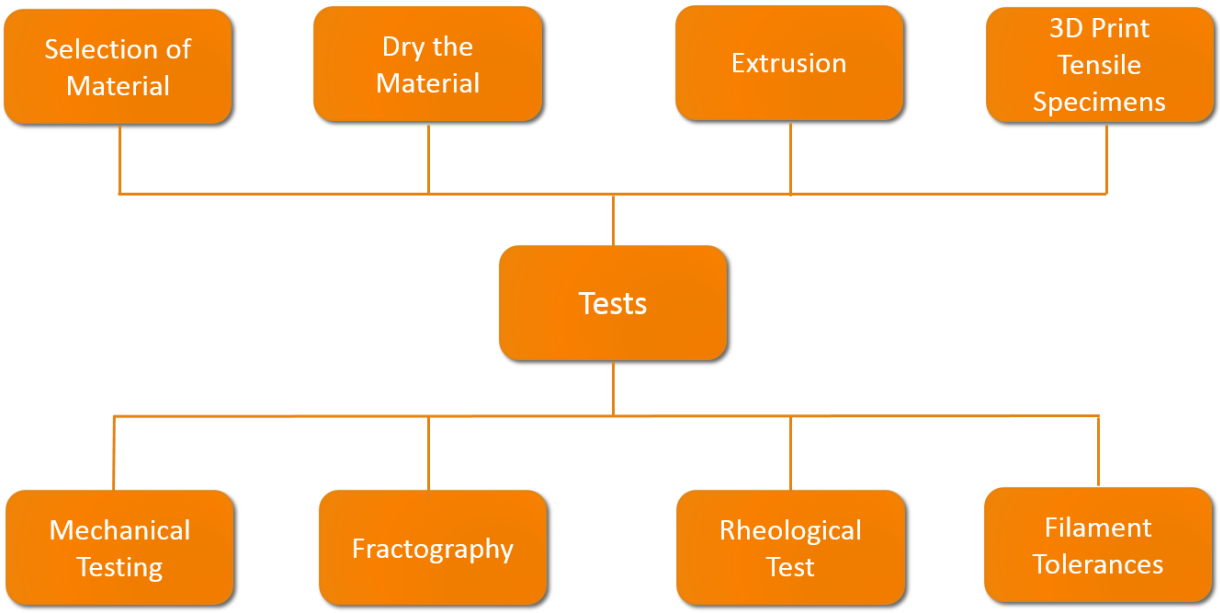

Figure 4.1.- Schematic of experimental procedure used during the investigation

4.1 Material Selection

The investigation consisted on common polymeric materials such as Styrene Ethylene Butadiene Styrene and Acrylonitrile Butadiene Styrene. The two materials were blended together in different ratios.

4.1.1 Acrylonitrile Butadiene Styrene

One of the materials used during this analysis, was Acrylonitrile Butadiene Styrene (ABS). It is classified as a common thermoplastic polymer, well known for its valuable properties such as high impact strength, toughness and good surface appearance. It is composed by three main monomers: acrylonitrile, butadiene and styrene (Figure 4.2). This thermoplastic has a wide range of applications, such as pipe fittings, automotive interior, and has become popular in FDM technologies [42].

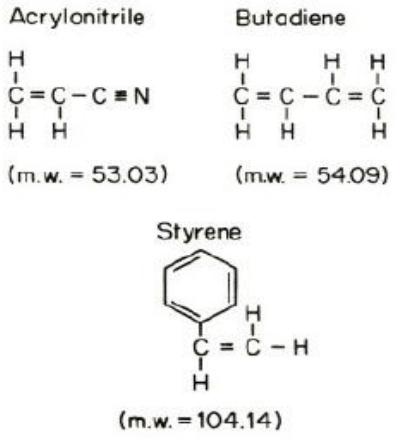

Figure 4.2.- Chemical structure of ABS [43]

4.1.2 Styrene Ethylene Butadiene Styrene

Styrene Ethylene Butadiene Styrene is an elastomer that is able to display large strains in response to stresses, it can be used as a replacement for rubber. It forms part of the family of styrenic block copolymers. This elastomer is easier to process as thermoplastics when heat is added. It is well known for its high strains and elongation ranges over 800%. Due to the properties that this elastomer possess, it is suitable for applications such as footwear, adhesives and sealants [44].

4.1.3 Polymeric Blends

The commercial ABS and SEBS materials that were used for this research investigation were: (1) ABS-MG94 produced by SABIC (Pittsfield, MA)under the Cyclolac TM product line; and (2) SEBS-g-MA FG1901-GT (Kraton, Houston, TX, USA) which its composition is combined with approximately a 1.4%-2.0% percentage of maleic anhydride. It is necessary to dry polymeric materials before extrusion, because they tend to absorb the humidity from the environment. For this reason the preparation of the monofilaments started by drying the resins on a compressed air dryer (Dri-Air CFAM Micro-Dryer, East Windsor, Connecticut, USA). Temperatures of drying varied for both resins: (1)ABS MG94 required a drying temperature of 80°C for a period of time of two hours; on the other hand, (2) SEBS-g-MA Kraton FG1901-GT was dried at a temperature of 60°C for one hour. All of the temperatures were based on manufacturer-supplied material data sheets, and literature research. After the materials were dried, they were extruded on a single-screw extruder Filabot EX2 (Barre, VT, USA) and a Dr. Collin twin-screw extruder/compunder (Model ZK 25 T, Dr. Collin GmbH, Eberseberg, Germany) (Figures 4.4 and 4.5). The five polymeric blends that were extruded using the two extrusion systems are listed in Table 4.1. Finally, it is important to mention that the same spooler and water bath was used for both extrusion systems, only the extrusion systems differed, this was with the intention to keep all the parameters the same except for the extruder systems.

Table 4.1. Compositions for ABS-MG94/SEBS-g-MA blends elaborated on a single-screw extruder and a twin-screw screw extruder.

Filabot EX2 single-screw extruder	**Dr. Collin twin-screw extruder**
ABSMG94 100%	ABSMG94 100%
ABSMG94: SEBS-g-MA 75:25	ABSMG94: SEBS-g-MA 75:25
ABSMG94: SEBS-g-MA 50:50	ABSMG94: SEBS-g-MA 50:50
ABSMG94: SEBS-g-MA 25:75	ABSMG94: SEBS-g-MA 25:75
ABSMG94: SEBS-g-MA 10:90	ABSMG94: SEBS-g-MA 10:90

Figure 4.4.-Polymer extrusion lab Dr. Collin twin-screw extruder/compounder

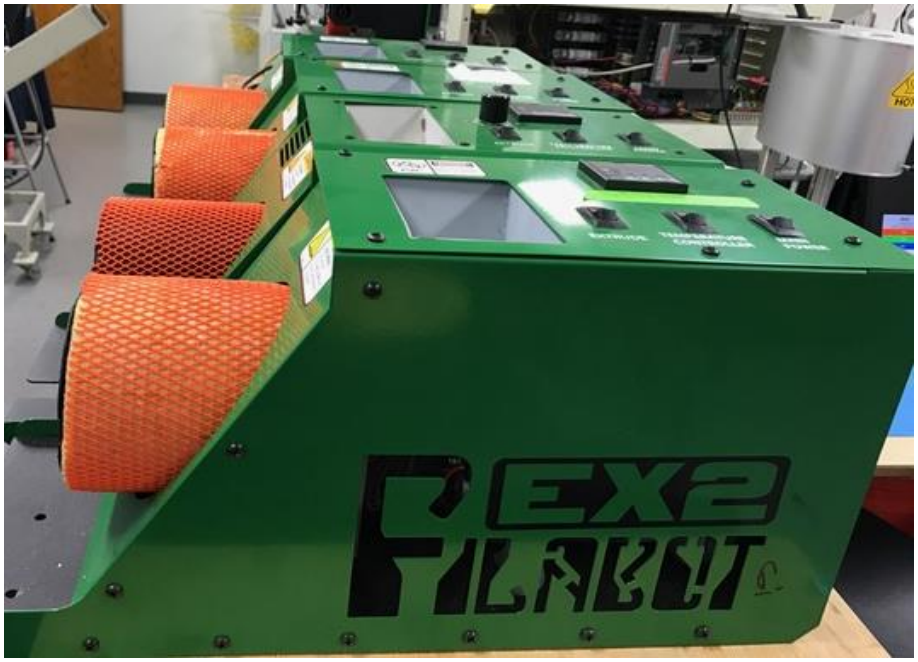

Figure 4.5.- Polymer extrusion Lab Filabot EX2 single-screw extruder/compounder

4.2 Extrusion

Extrusion temperatures and pressures on the Dr. Collin twin-screw extruder/compounder varied depending on the ratios of the material. Table 4.2 lists in detail the parameters used to extrude the polymeric blends on the twin-screw extruder. On the other hand, the extrusion process was simpler for the single-screw system; because there was only one temperature zone. The only controllable variable was the temperature. Instead, the parameters that were needed to take care of for the single-screw extruder were: extrusion temperatures and the diameter size required to feed the desktop printer. The different temperatures used in for the Filabot extruder are represented in table 4.3; as noticed, the increase in temperatures is required as the incorporation of SEBS increases in the polymeric matrix in order to favor mixing of both polymers [45]. In addition, the diameter sizes from each extrusion differ, the die diameter for the single-screw extruder is 2mm; whereas the die diameter for the twin-screw extruder is 3mm.

Table 4.2. Extrusion parameters for the ABS-MG94/SEBS-g-MA blends extruded with the Dr. Colling twin-screw extruder compounder.

Material **ABS : SEBS**	**Temp. zone 1 (◦C)**	**Temp. zone 2 (◦C)**	**Temp. zone 3 (◦C)**	**Temp. zone 4 (◦C)**	**Temp. zone 5 (◦C)**	**Temp. zone 6 (◦C)**	**RPM main**	**Pressure main screws**	**Melt pump pressure**
100 : 0	200	210	210	210	200	190	28	90	54
75 : 25	200	210	210	210	200	190	28	90	48
50 : 50	200	210	215	215	210	195	33	90	34
25 : 75	200	210	215	215	210	195	36	90	39
10 : 90	200	210	215	215	210	195	39	90	40

Table 4.3. Extrusion parameters for the ABS-MG94/SEBS-g-MA blends extruded with the Filabot maker single-screw extruder compounder.

Material **ABS : SEBS**	**Extrusion Temperature (°C)**
100 : 0	210
75 : 25	210
50 : 50	215
25 : 75	215
10 : 90	215

4.3 Tensile Specimens

Specimens were fabricated, through the use of a desktop 3D printer; Lulzbot Taz 5 (Aelph Objects Inc, Loveland, Colorado USA). In order to perform tensile testing, the specimens were printed following specifications of Type V ASTM-638. All of the specimens were printed using a nozzle diameter of 0.6mm (Figure 4.6).

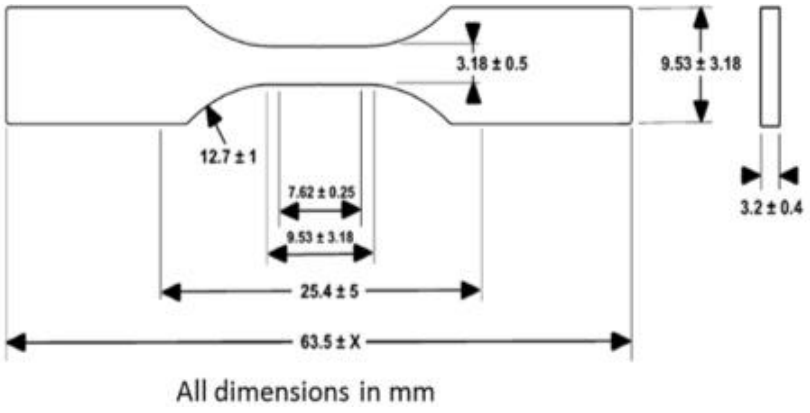

Figure 4.6.-Type V specimen dimensions [45]

As previously mentioned, tensile specimens were 3D printed with five polymeric blends (Table 4.1) using three raster angles on a XYZ plane. These raster angles consisted on: 0°/90°, +45°/-45° and 90°, with a 100% infill and raster height of 0.27mm (Figure 4.7). Printing temperatures varied, depending on each material as shown in Table 4.4. As indicated in table 4.4 the temperatures increased from 230°C to 295°C as the percentage of SEBS increased in the polymer matrix. The parameters of printing were maintained the same for all of the extruded monofilaments by the two extrusion systems.

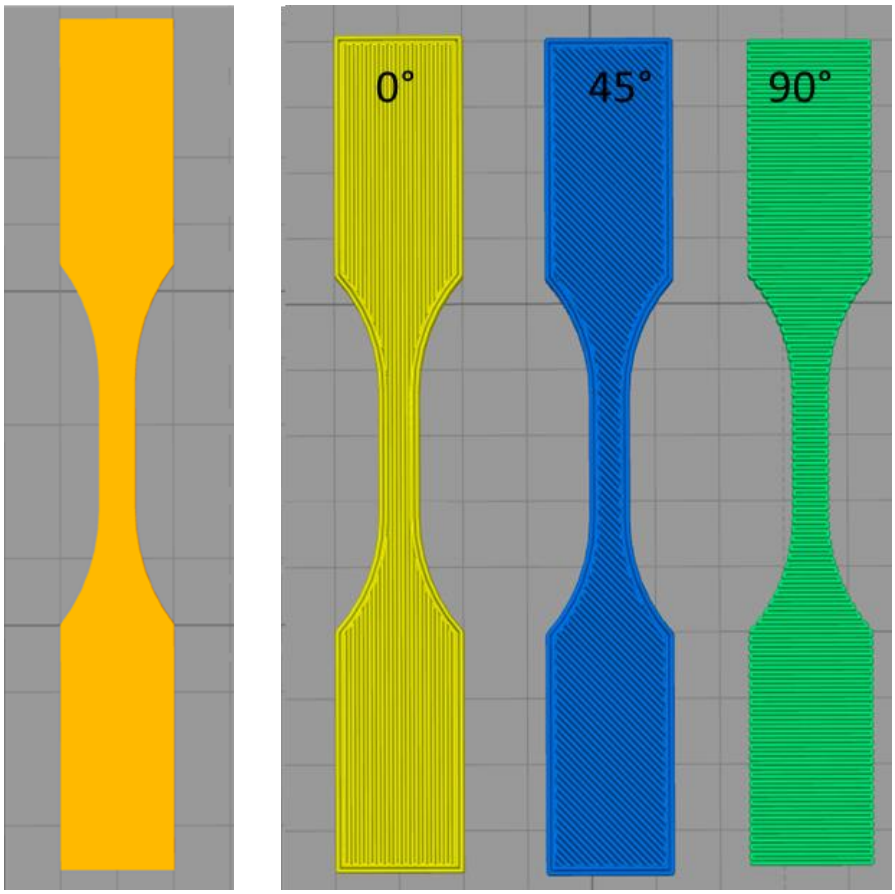

Figure 4.7.- Tensile specimen design with different raster angles

Table 4.4. Printing parameters for the ABS-MG94/SEBS-g-MA blends extruded with single-screw extruder and twin-screw extruder compounder.

MATERIAL ABS : SEBS	NOZZLE TEMPERATURE	BED TEMPERATURE
100 : 0	230	110
75 : 25	250	110
50 : 50	250	110
25 : 75	260	110
10 : 90	295	110

4.4 Tensile Test

Tensile testing was executed by the use of an Instron 5866 (Instron, Norwood, Massachusetts, USA) tensile testing machine equipped with a 10kN load cell, and a speed of 10mm/min with a temperature of 24°C as indicated in the ASTM D638-10 [46].

A quantity of ten tensile specimens were printed and tested (Figure 4.8). The test was carried out for each of the polymer blends that were extruded. A comparison of stress, strain and Young's modulus results were obtained and compared among the different extrusion systems and raster angles used for the study (Figure 4.9).

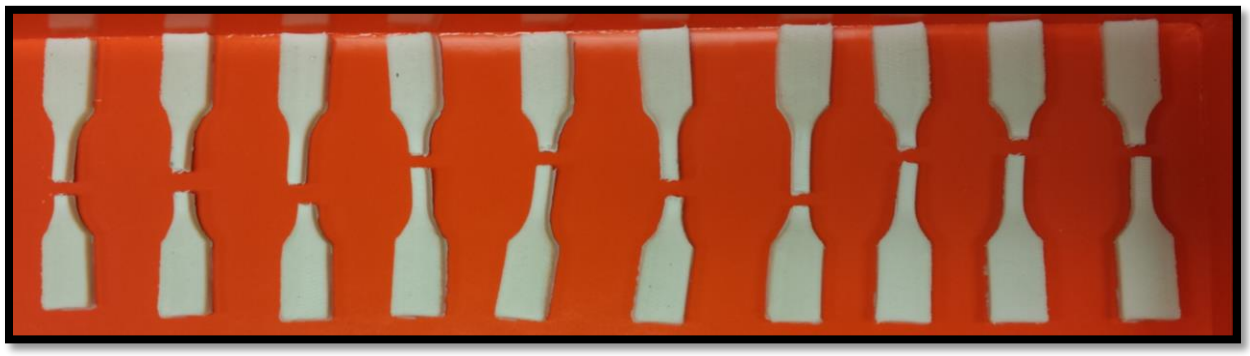

Figure 4.8.- Tensile specimens 3D printed for tensile test

4.5 Rheological Test

The rheological test was achieved by the use of a Tinius Olsen MP1200 melt flow indexer (Tinius Olsen, Horsham, Pennsylvania, USA). The test was conducted following ASTM D1238-13 standard (procedure A) [47]. Melt flow index is a technique that measures the weight of a polymer that is able to flow through a die of the instrument for a certain period of time. In order for the polymer to flow there are two parameters to take into account: weight and temperature (Figure 4.9). The weight will be in charge to produce a force, which creates the flow in the system. Temperature on the other hand, will melt the polymer that is inside, for this reason temperature is

dependent on the material that is being tested. Based on the ASTM standard, approximately 7g of each blend were placed in pellet form into the instrument, followed by a weight load of 3.8g. The temperature used to melt all the samples was 230°C, and each sample was melted for a period of ten minutes. After those ten minutes samples were collected and weighted. The measured weights were recorded by the instrument and this one was able to provide final records with respect to the amount in grams, collected in ten minutes.

Figure 4.9.- Polymer Extrusion Lab Melt Flow Index instrument

4.6 Filament Tolerances

The diameter of each of the filaments was measured in order to observe the precision of the extrusion process. A length of 50cm was taken for each of the filaments were five measurements from the diameters were taken, in order to observe the consistency of the diameter size throughout the filament. Averages and standard deviations were calculated for each diameter of the filaments with their respective system of extrusion.

4.7 Fractography

Finally, a fractography study was performed by using a Hiachi TM-1000 scanning electron microscope (SEM; Hitachi High-Technologies Europe GmbH, Germany) to analyze the fracture surfaces of each tensile specimen. The surface from the samples tested were gold coated with a JEOL Smart Coater (JEOL, Peabody, MA, USA). This sample preparation was performed to reduce electron charging because the samples were non-conductive. The study aided the understanding of failure modes from all the elastomeric blends according to the raster orientation and blend ratios applied.

Chapter 5: Results

5.1 Tensile Testing Results

The main metric for this study was tensile testing of 3D printed test specimens. In this section, tensile test results are presented for each extrusion process with their respective raster orientation used. The results will be presented and discussed in the following order:

-Five blends with raster orientation of +45°/-45°: UTS and strain at break

- Five blends with raster orientation 0°/90°: UTS and strain at break

- Five blends with raster orientation 90°: UTS and strain at break

5.1.1 Comparison of +45°/-45° raster angle between two extruder systems

The ultimate tensile stress (UTS) results obtained by the use of five polymeric blends are displayed in Figure 5.1. As the percentage of SEBS in the polymeric matrix was increased the UTS decreased, this trend was the same for the two extrusion systems. However, the results are different when the two process of extrusion are compared. The graph seen in Figure 5.1, clearly shows that the UTS values are slightly lower in three of the blends extruded with the single-screw extruder compared to values from the blends fabricated in the twin-screw extruder. In the case of 100% ABS-MG94 and 25% SEBS-ABS, values were 1-4% higher for filaments extruded with the Filabot to those with the Collin not a significant difference. In the case of blends containing 50%-90% SEBS-ABS the difference in between values was greater ranging from 13%-39% of difference, where the twin screw extruder (Collin) had predominance with higher values compared to the single screw-extruder (Filabot). The trend for both extrusion systems behaved the opposite for the tensile strain values compared to the ones for the ultimate tensile stress. Values increased as the percentage of SEBS increases in the polymeric matrix; these increase in values was observed for the two extrusion systems. This can be understood by the fact the percentage or amount of SEBS

is increasing into the matrix producing a more elastic blend, thus increasing the percent elongation in the system. Comparing the two extrusion systems, the twin-screw extruder demonstrated larger % elongation values compared to those provided by the single-screw extrusion system. It can be demonstrated that the percentage difference was high especially for percentages of 50%, and 75% SEBS-ABS with a percent difference of 52% and 78% respectively.

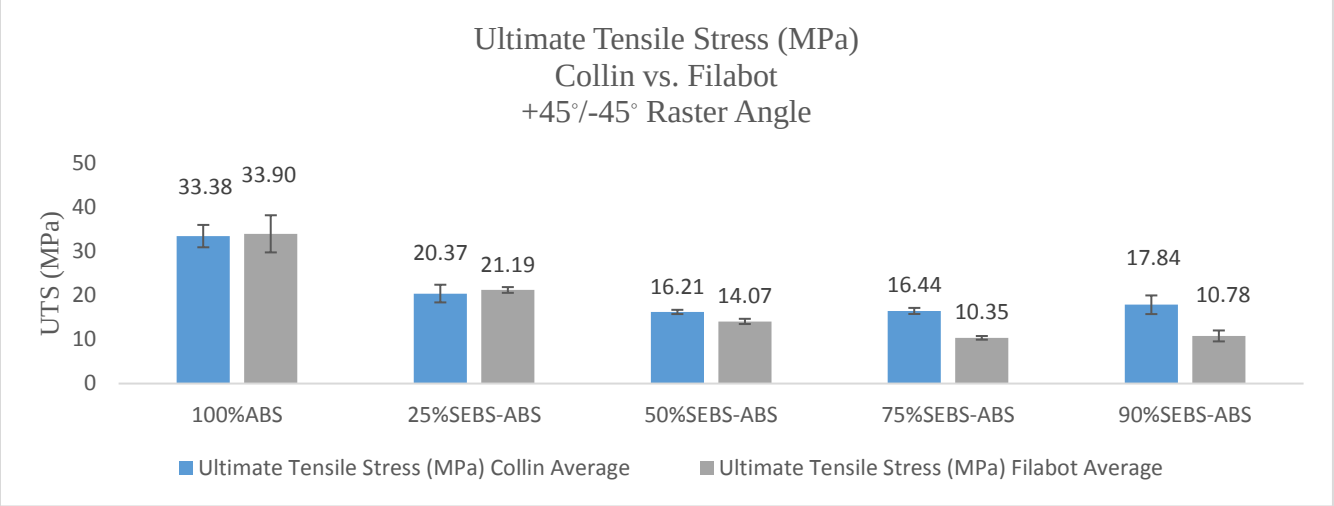

Figure 5.1.- UTS of single and twin screw-extruder systems with a raster angle of +45°/-45°

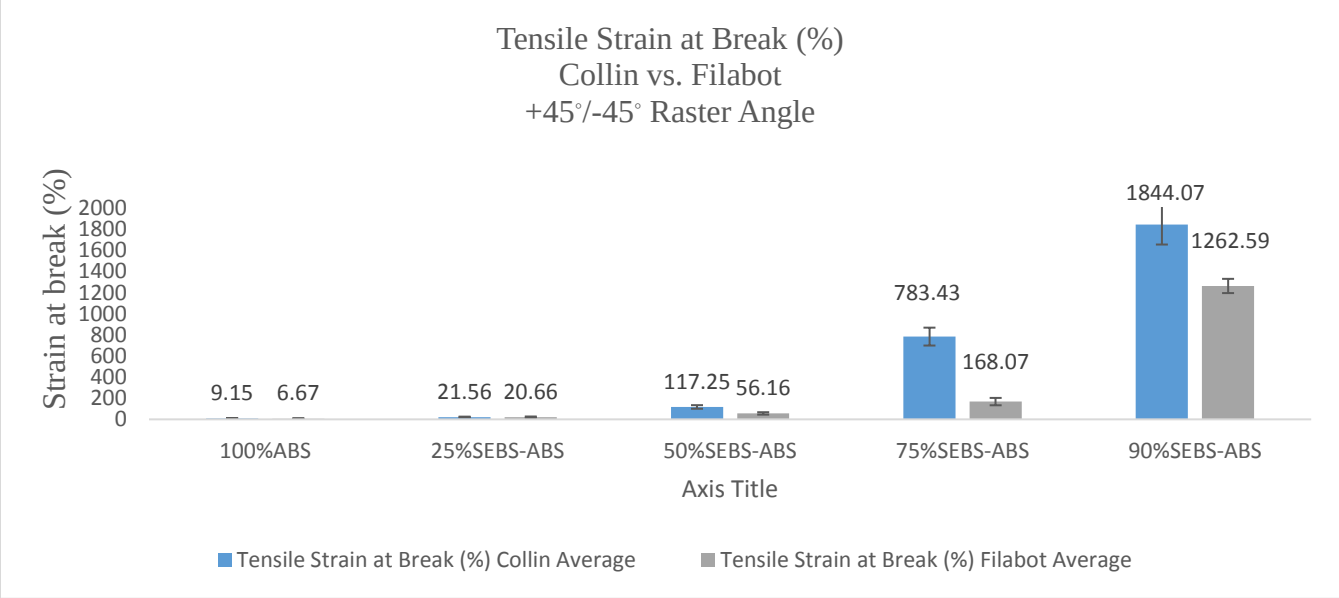

Figure 5.2.- Tensile Strain of single and twin-screw extruder systems with a raster angle of +45°/45°

5.1.2 Stress-strain curves

The following graphs are representative stress-strain curves obtained from tensile specimens that were 3D printed using a +45/-45 raster angle. Figure 5.3 illustrates the behavior of single-screw extruded tensile specimens. On the other hand, Figure 5.4 illustrates the behavior of twin-screw extruded tensile specimens.

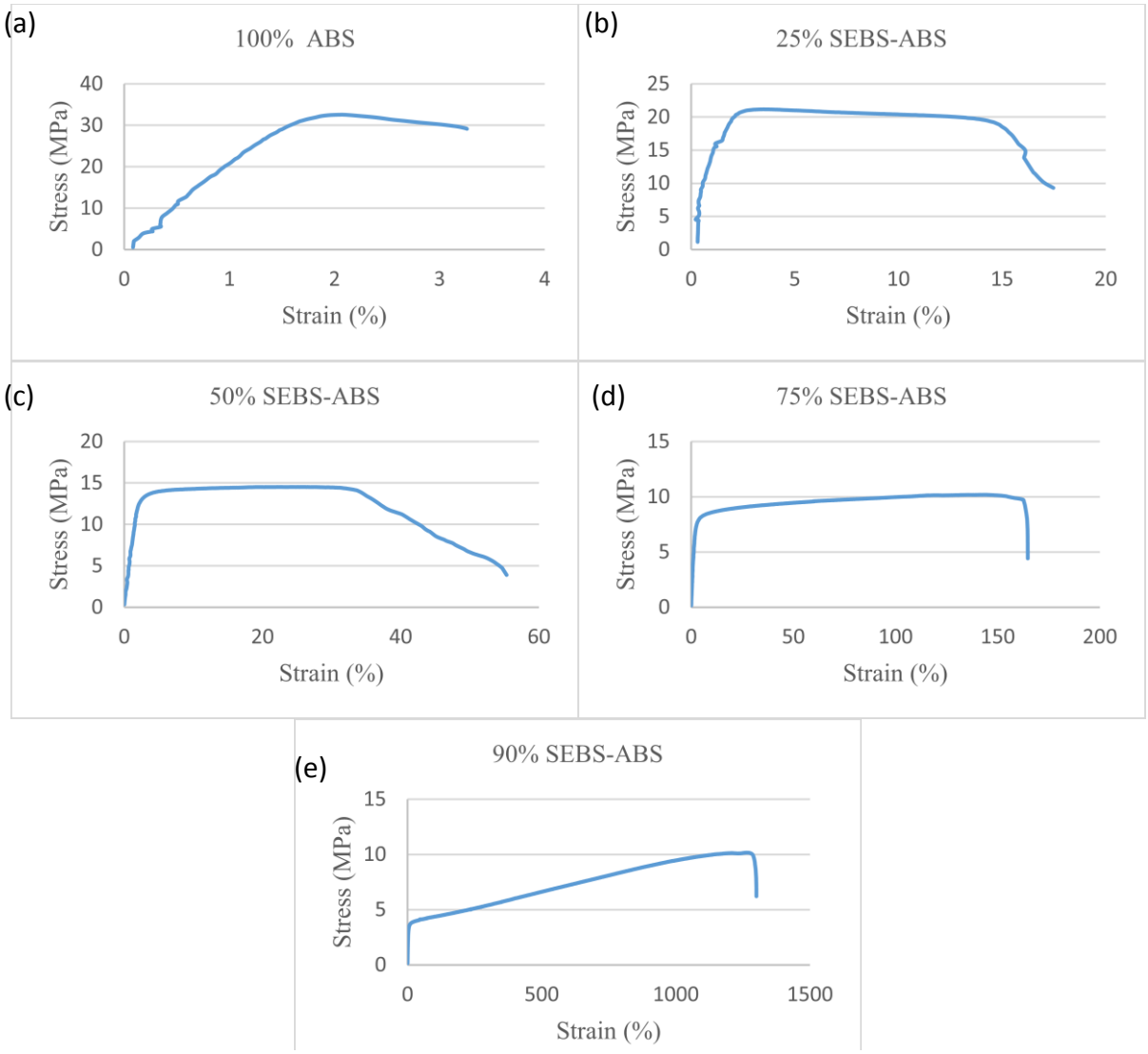

Figure 5.3.- Representative stress-strain curves of rubberized blends with a raster patter of +45°/45° single-screw extruder. (a) 100% ABS, UTS = 32.56, %El = 3.25; (b) 25% SEBS-ABS, UTS = 21.17, %El = 17.48; (c) 50% SEBS-ABS, UTS = 14.52, %El = 55.32; (d) 75% SEBS-ABS, UTS = 10.19, %El = 164.64; (e) 90% SEBS-ABS, UTS = 10.17, %El = 1300.21.

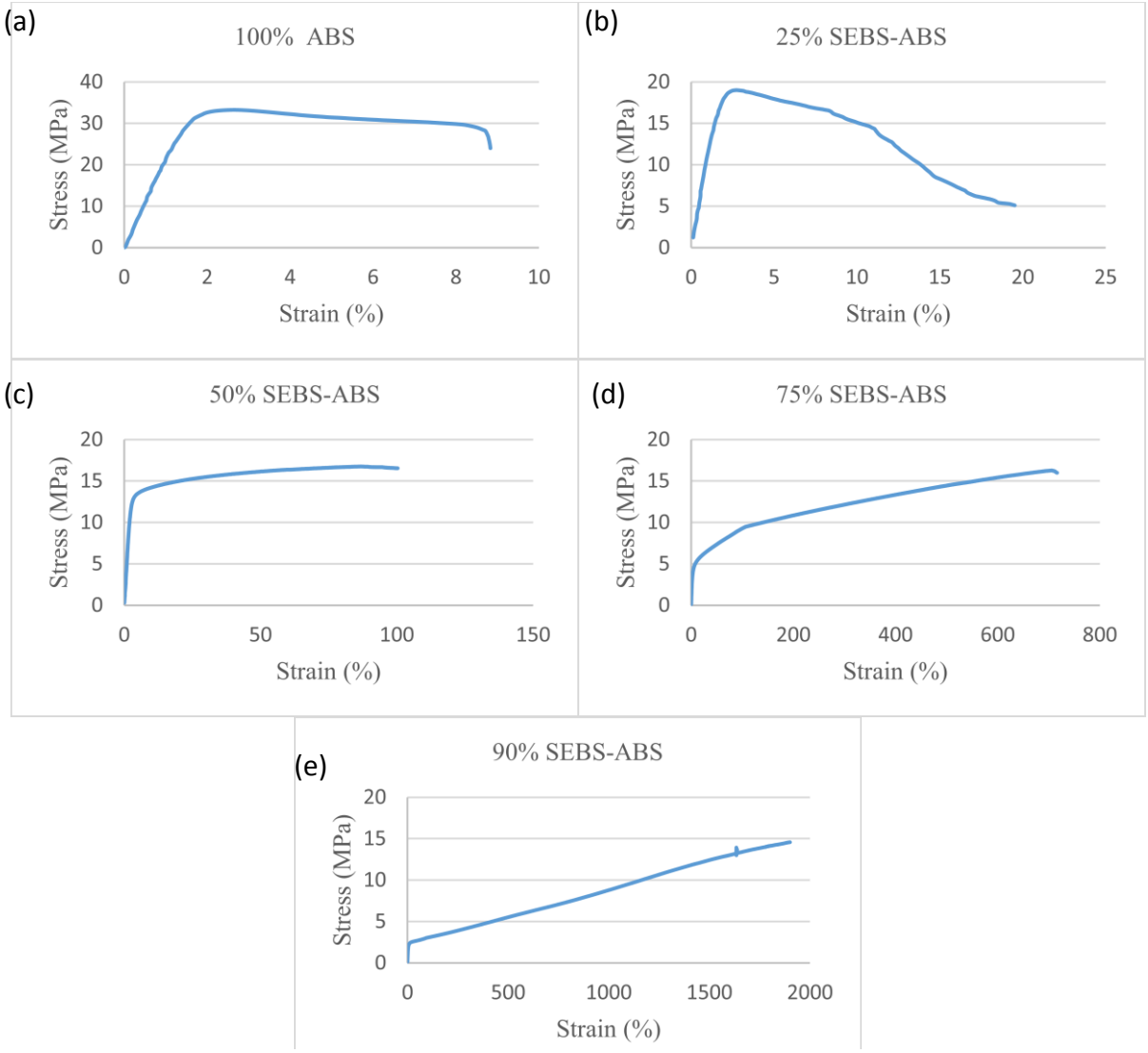

Figure 5.4.- Representative stress-strain curves of rubberized blends with a raster patter of +45°/45° twin-screw extruder. (a) 100% ABS, UTS = 33.25, %El = 8.71; (b) 25% SEBS-ABS, UTS = 19.01, %El = 21.80; (c) 50% SEBS-ABS, UTS = 16.76, %El = 115.81; (d) 75% SEBS-ABS, UTS = 16.28, %El = 722.30; (e) 90% SEBS-ABS, UTS = 14.71, %El = 1915.16.

5.1.3 Comparison of 0°/90° raster angle between two extruder systems

Interpreting the ultimate tensile stress results for the 0°/90° raster angle (Figure 5.5 and 5.6), it can be observed that the trend decreases within the addition of SEBS in the matrix as it was presented on results analyzed in section 5.1.1. The decrease of UTS values occurs in both systems of extrusion, when relating these two. It is presented that values of twin-screw extruder system have to some extent predominance in contrast to the single-screw extruder systems. The UTS stress results are close to each extrusion system for percentages of 100% ABS-MG94, 25% SEBS-ABS and 50% SEBS-ABS. Percentages of 75% SEBS-ABS and 90%SEBS-ABS demonstrated higher dissimilarity in between values, the percent variance was 29% and 27% respectively.

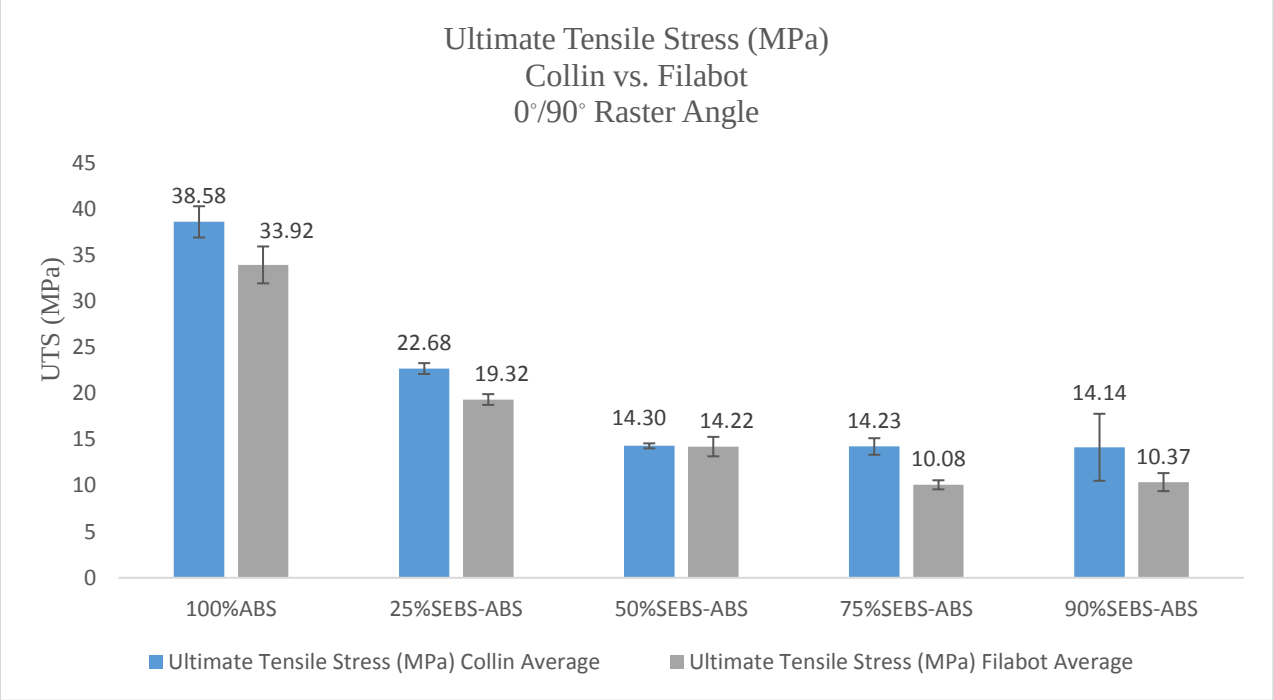

Figure 5.5.- UTS of single and twin-screw extruder systems with a raster angle of 0°/90°

On the other hand, tensile strain at break indicated that the addition of SEBS also has an impact in the recorded results (Figure 5.6). The trend for this raster angle showed that the strain is increased as the percentage of SEBS increases, this is showed for both extrusion systems as well. The greater differences in values were for the percentages of 75% and 90% SEBS, an average of 28% of difference among values is present for these to blends in between the extrusion systems. However, for all of the polymeric blends that were extruded in the twin-screw extrusion system, had higher tensile strain values. It is noticeable that not only the effect of extrusion systems made a difference with respect to results, but the raster angle that was used.

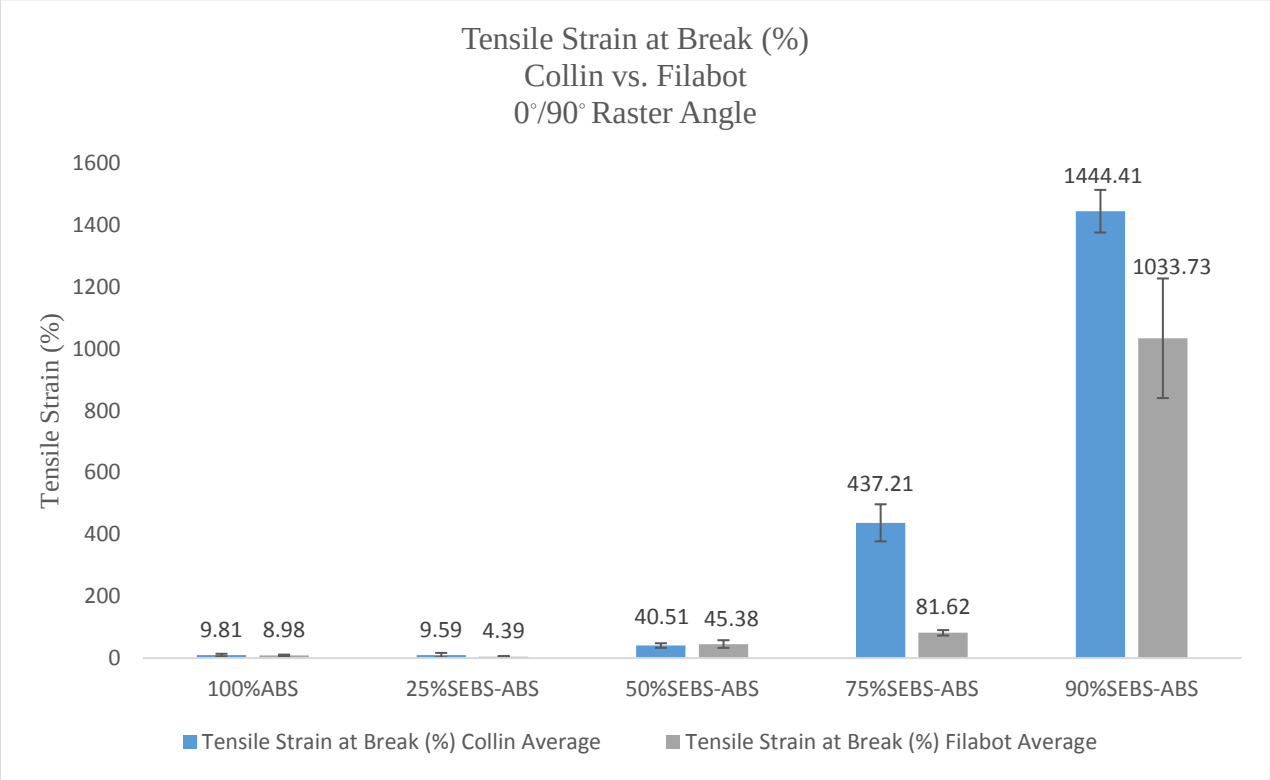

Figure 5.6.- Tensile Strain of single and twin-screw extruder systems with a raster angle of 0°/90°

5.1.4 Stress-strain curves

The following graphs are representative stress-strain curves obtained from tensile specimens that were 3D printed using a 0°/90°raster angle. Figure 5.7 illustrates the behavior of single-screw extruded tensile specimens. On the other hand, Figure 5.8 illustrates the behavior of twin-screw extruded tensile specimens.

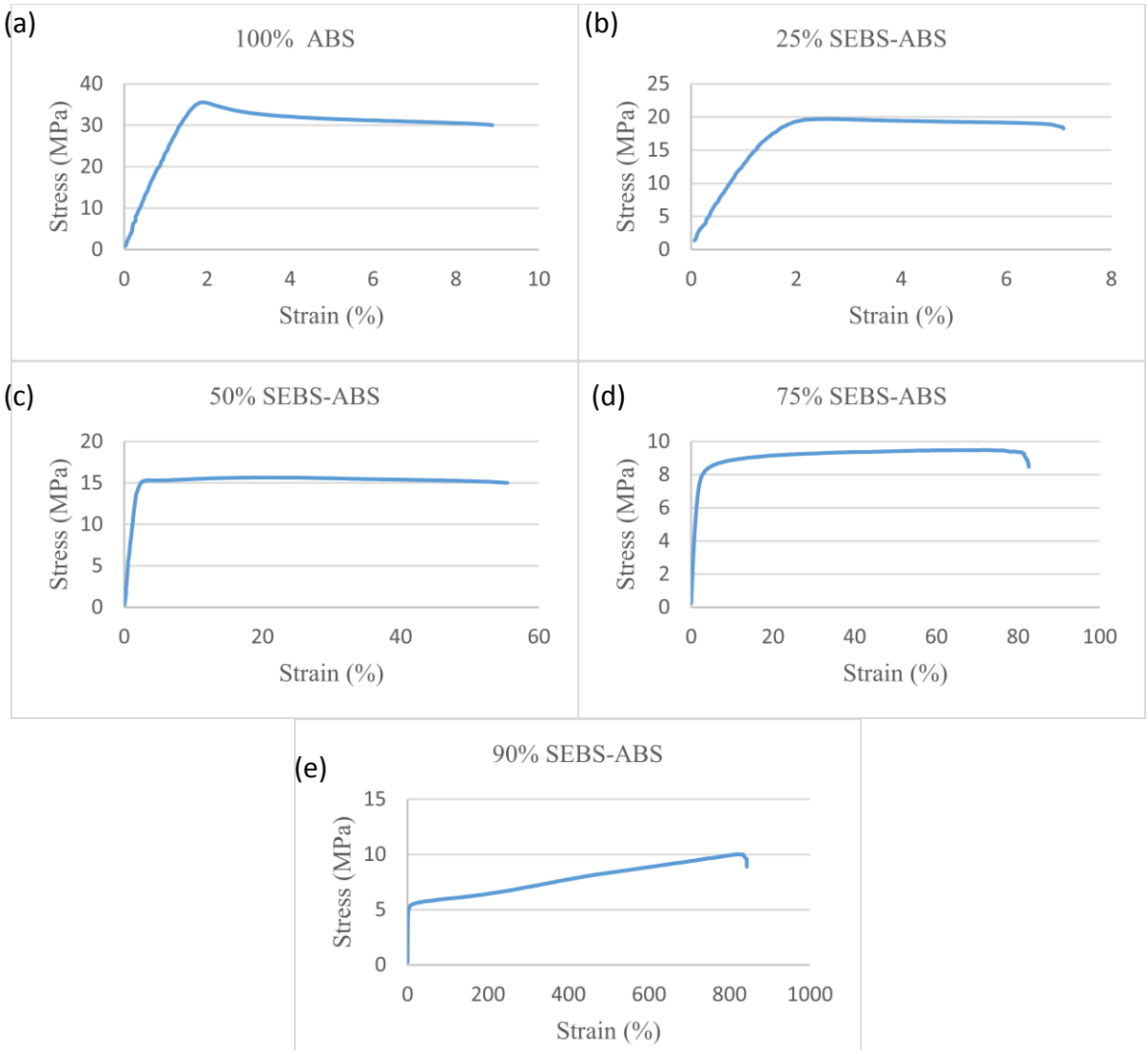

Figure 5.7.- Representative stress-strain curves of rubberized blends with a raster angle of 0°/90° single-screw extruder. (a) 100% ABS, UTS = 34.31, %El = 10.71; (b) 25% SEBS-ABS, UTS = 19.69, %El = 4.47; (c) 50% SEBS-ABS, UTS = 13.93, %El = 52.65; (d) 75% SEBS-ABS, UTS = 9.50, %El = 81.29; (e) 90% SEBS-ABS, UTS = 10.03, %El = 842.87.

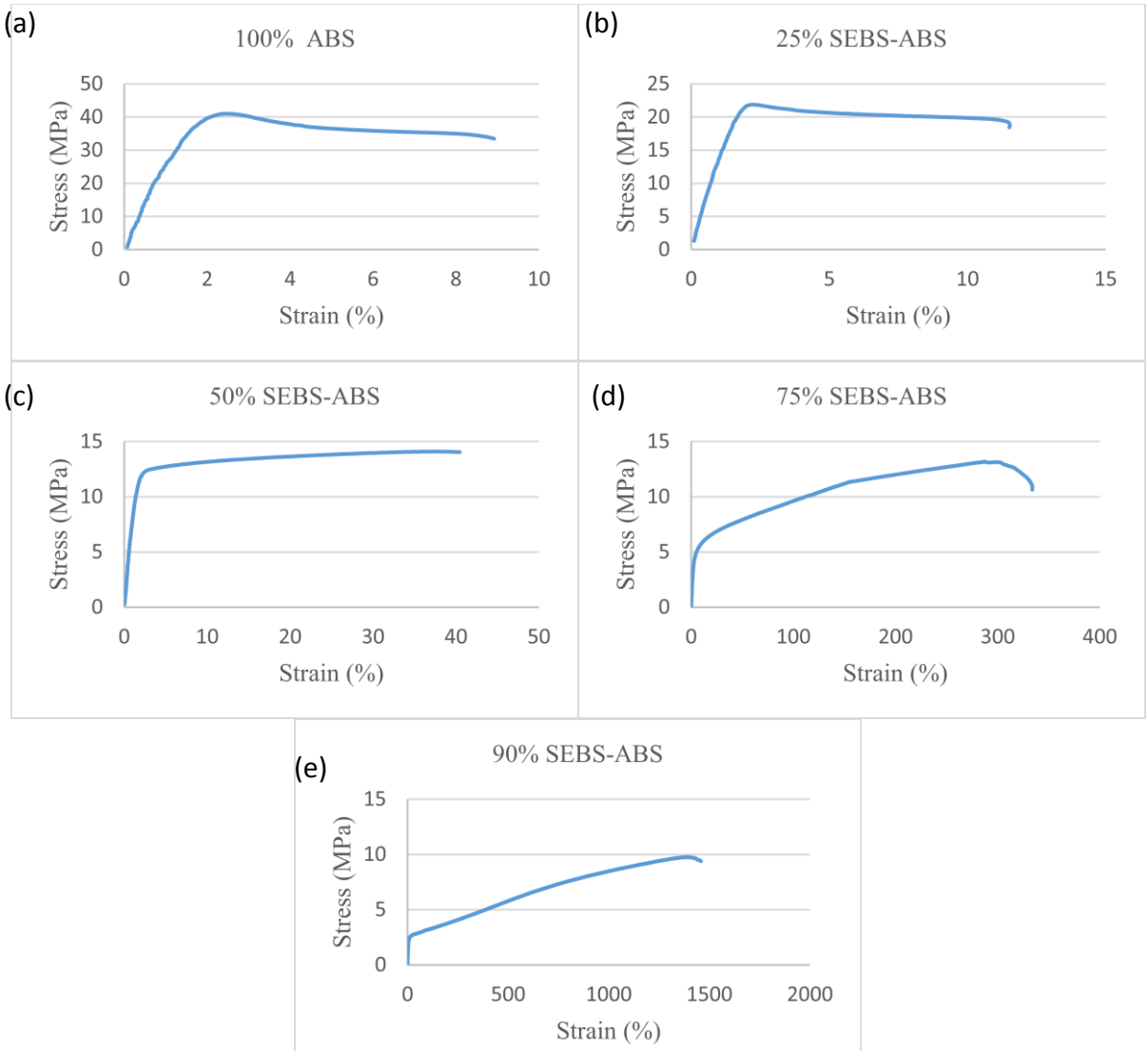

Figure 5.8.- Representative stress-strain curves of rubberized blends with a raster angle of 0°/90° twin-screw extruder. (a) 100% ABS, UTS = 40.99, %El = 8.92; (b) 25% SEBS-ABS, UTS = 21.86, %El = 10.39; (c) 50% SEBS-ABS, UTS = 14.10, %El = 40.13; (d) 75% SEBS-ABS, UTS = 13.18, %El = 333.72; (e) 90% SEBS-ABS, UTS = 10.61, %El = 1475.70.

5.1.3 Comparison of 90° raster angle between two extruder systems

In 3D printing, the raster angle of 90° is also known as Faux Vertical (FV), this one mimics the actual vertical direction of printing, instead of be printed on the XYZ direction it is printed on the XYZ but using a 90° angle [48]. The decrease in UTS trend that has been present on section 5.1.1 and 5.1.2 is followed up on the last raster angle for this study. However, values in blends containing 50%, 75% and 90% SEBS-ABS were much lower values compared to the +45°/-45° and 0°/90° degree raster angle. The values obtained for this specific raster angle showed the highest difference for the 75% SEBS-ABS showing a difference of 33% lower, using the single-screw extruder compared to the twin-screw extruder. The rest of the values did not show that much of a difference in between values.

The results for the tensile strain for this raster angle followed the trend of the previous raster angles analyzed. However, the predominance of the use of the twin-extruder system made a bit difference for values of polymeric blends containing 50%, 75% and 90% SEBS-ABS. Approximately, a decrease of 14% in blends of 50% and 75% SEB-ABS was reported for tensile strain results, using the single-screw extruder system. On the other hand, the greatest variance was the one in the 90% SEBS-ABS amongst all the values obtained from this test. Values showed a decrease of 52% of the strain at break with the use of the Filabot extruder compared to the Collin extruder.

Overall, the filaments extruded with the single-screw extruder were not favored, in the case of tensile specimens printed using faux vertical as the raster angle. Values decreased within the increment of the elastomer in the polymeric matrix. In addition, comparing the mechanical testing in all the raster angles acquired, the use of the Collin extruder provided higher values for all the blends. However, it is noticeable that as the addition of SEBS increases especially after 50%SEBS-

ABS blends, the mechanical properties from the blends extruded in the Filabot decreases drastically in tensile strain, approximately 50% less than the values provided by the blends extruded in the Collin extruder.

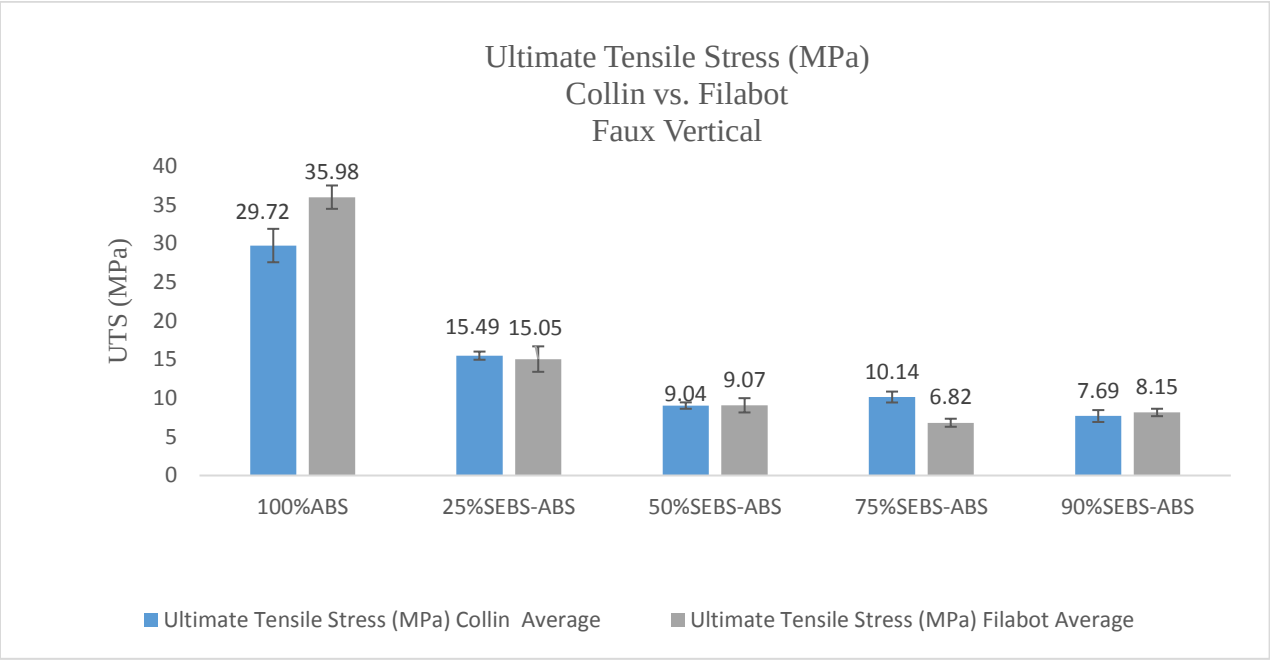

Figure 5.9.- UTS of single and twin-screw extruder systems with a raster angle of 90°

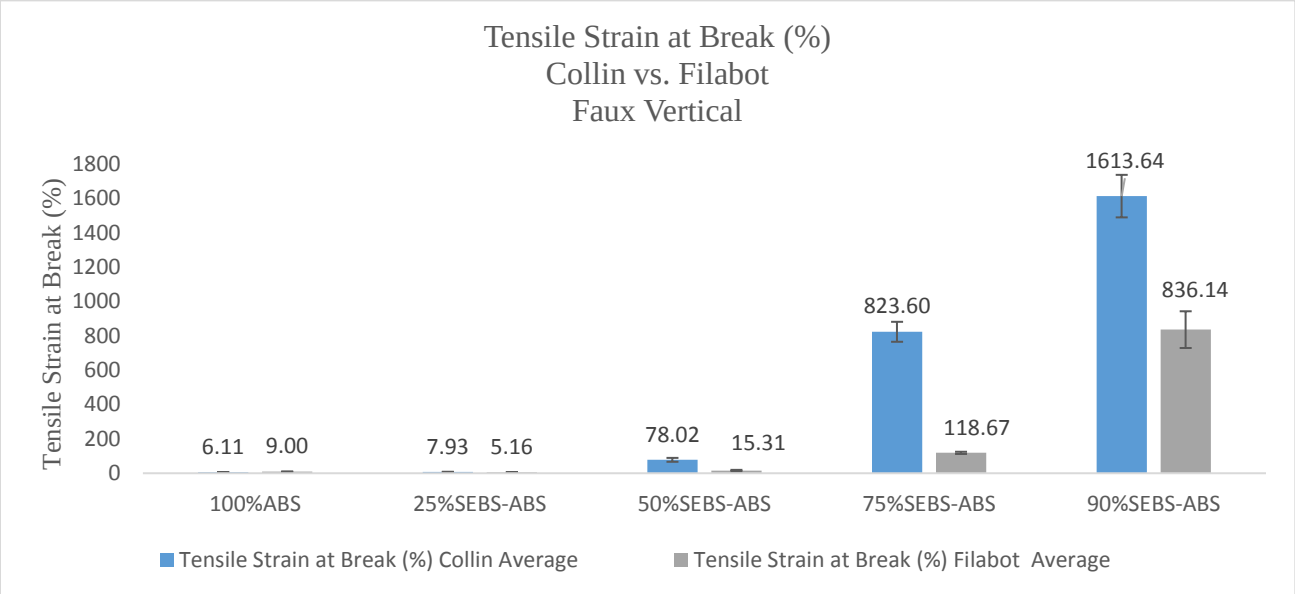

Figure 5.10.-Tensile Strain of single and twin-screw extruder systems with a raster angle of 90°

5.1.4 Stress-strain curves

The following graphs are representative stress-strain curves obtained from tensile specimens that were 3D printed using a faux vertical raster direction. Figure 5.11 illustrates the behavior of single-screw extruded tensile specimens. On the other hand, Figure 5.12 illustrates the behavior of twin-screw extruded tensile specimens.

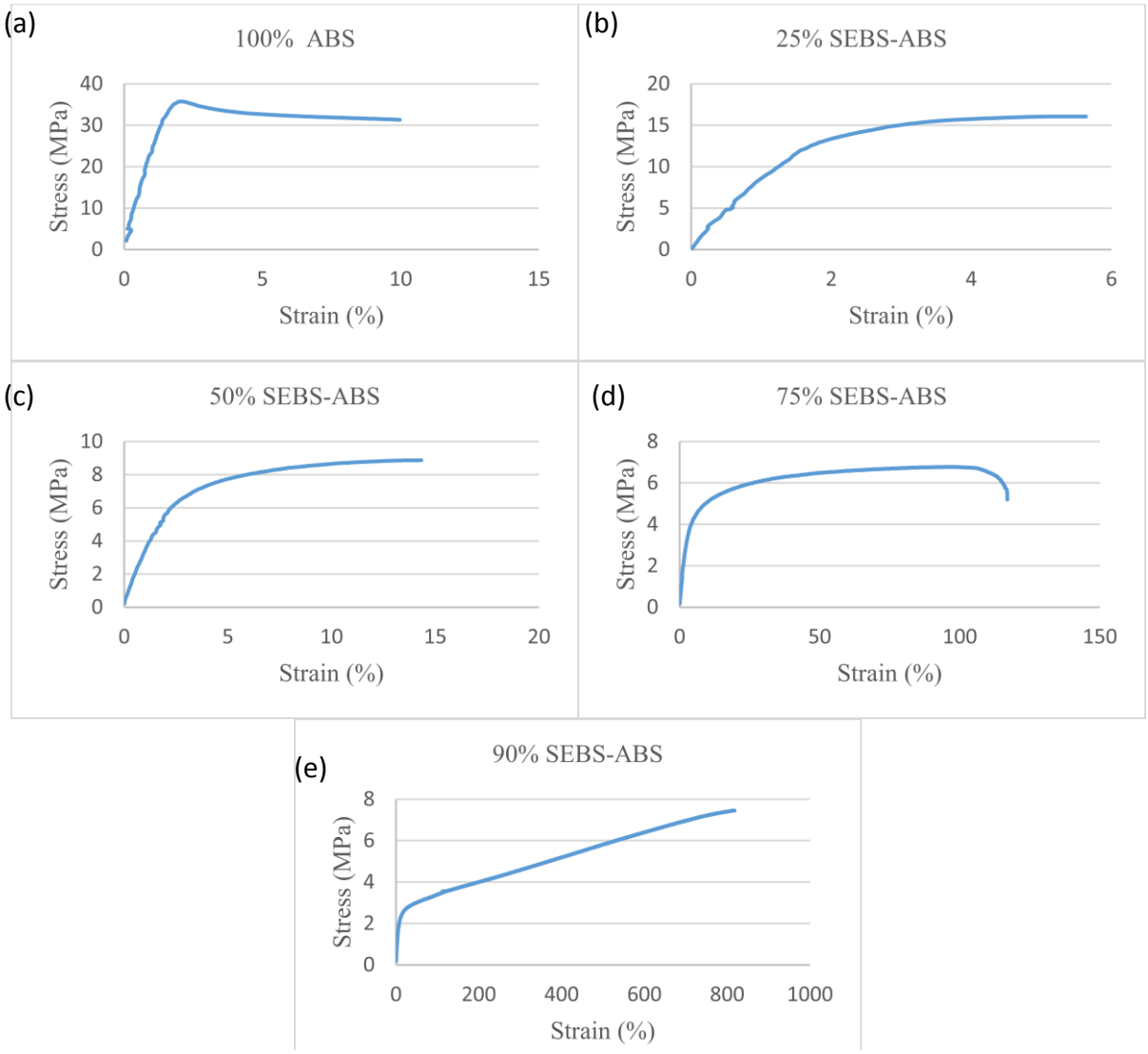

Figure 5.11. - Representative stress-strain curves of rubberized blends with a faux vertical raster orientation (raster angle of 90°) single-screw extruder. (a) 100% ABS, UTS = 34.22, %El = 8.92; (b) 25% SEBS-ABS, UTS = 14.08, %El = 5.53; (c) 50% SEBS-ABS, UTS = 8.87, %El = 16.84; (d) 75% SEBS-ABS, UTS = 6.78, %El = 116.81; (e) 90% SEBS-ABS, UTS = 7.46, %El = 826.45.

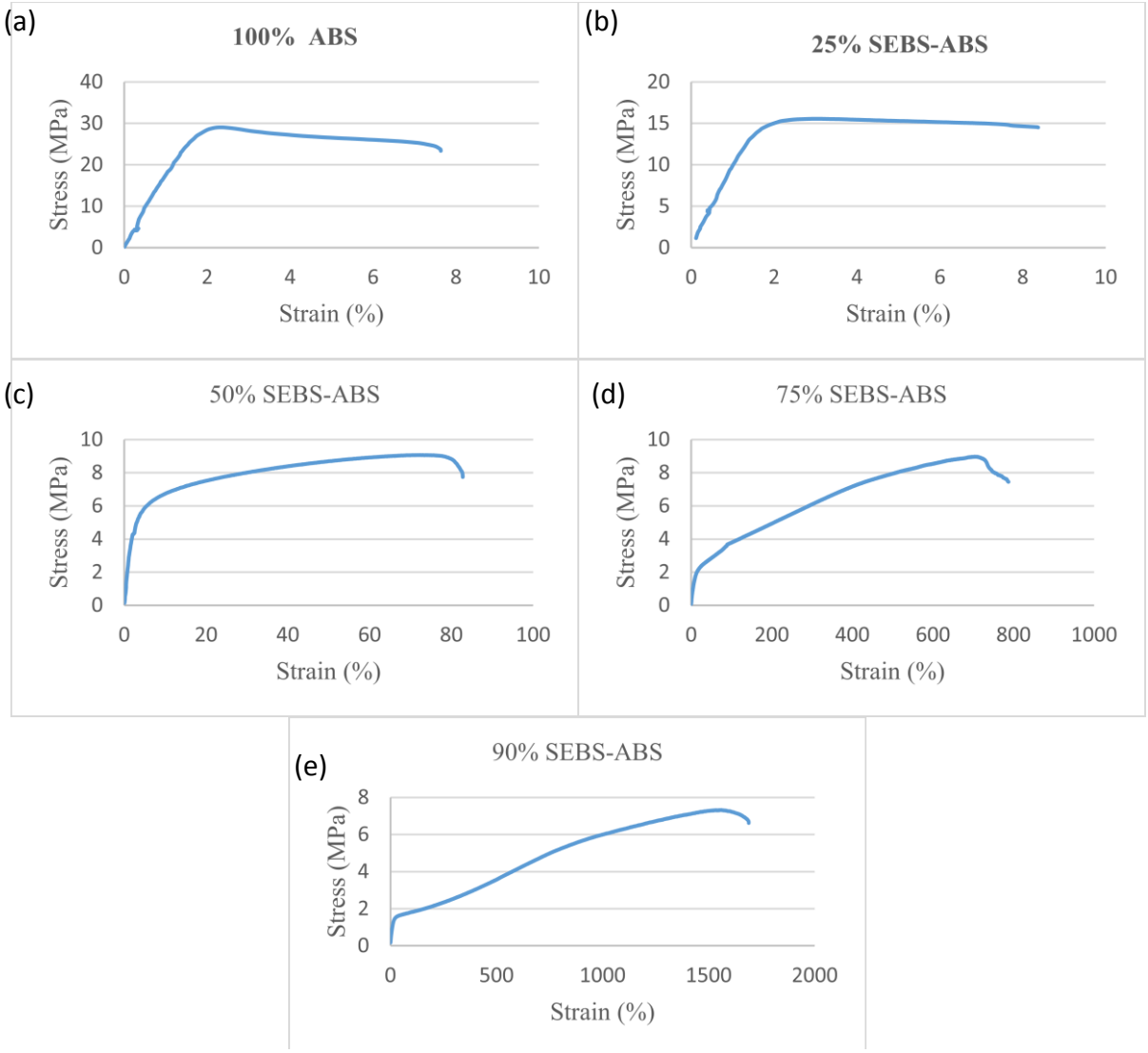

Figure 5.12. - Representative stress-strain curves of rubberized blends with a faux vertical raster orientation (raster angle of 90°) twin-screw extruder. (a) 100% ABS, UTS = 29.05, %El = 7.50; (b) 25% SEBS-ABS, UTS = 15.55, %El = 7.77; (c) 50% SEBS-ABS, UTS = 9.09, %El = 82.66; (d) 75% SEBS-ABS, UTS = 10.21, %El = 814.83; (e) 90% SEBS-ABS, UTS = 7.32, %El = 1688.83.

5.1.4 Polymeric blends extruded with a twin-screw extrusion system

During the last sections comparison, in between each polymeric blend was made with the respective raster angle as well as the system of extrusion used. This section will be intended from mechanical testing results using the twin-screw extrusion system. Table 5.1 contains a summary of the results acquired for each polymeric blend and the raster angle used during the analysis. Beginning with 25% SEBS-ABS, UTS was dominated by the 0°/90° raster angle. It was not the same case for the tensile strain though, raster angle of +45°/-45° was the one with higher tensile strain.

Table 5.1. Tensile test results from monofilaments extruded on the twin-screw extruder along with their respective printed raster orientation.

MATERIAL	YOUNG'S MODULUS (MPA)	ULTIMATE TENSILE STRESS (MPA)	TENSILE STRAIN AT BREAK (%)
	Average (Collin)	**Average(Collin)**	**Average (Collin)**
25%SEBS-ABS			
+45°/-45°	1542.52 ± 346.31	20.37 ± 2.00	21.56 ± 4.09
0°/90°	1657.84 ± 253.72	22.68 ± 0.59	9.59 ± 7.22
90°	1166.15 ± 202.75	15.49 ± 0.53	7.93 ± 0.72
50%SEBS-ABS			
+45°/-45°	616.54 ± 62.87	16.21 ± 0.48	117.25 ± 16.89
0°/90°	853.84 ± 61.99	14.30 ± 0.27	40.51 ±7.37
90°	238.33 ± 32.63	9.04 ± 0.41	78.02 ± 11.33
75%SEBS-ABS			
+45°/-45°	153.78 ± 28.05	16.44 ± 0.69	783.43 ± 84.74
0°/90°	168.69 ± 33.93	14.23 ± 0.90	437.21 ± 59.93
90°	17.62 ± 7.01	10.14 ± 0.70	823.60 ± 59.18
90%SEBS-ABS			
+45°/-45°	29.45 ± 26.49	17.84 ± 2.11	1844.07 ± 189.10
0°/90°	27.65 ± 14.40	14.14 ± 3.63	1444.41 ± 68.98
90°	5.88 ± 3.21	7.69 ± 0.77	1613.64 ± 123.85
100%ABS			
+45°/-45°	2374.25 ± 187.56	33.38 ± 2.53	9.15 ± 2.58
0°/90°	3002.00 ± 405.03	38.58 ± 1.69	9.81 ± 4.15
90°	2022.59 ± 127.37	29.72 ± 2.16	6.11 ± 1.16

Results for the 50% SEBS-ABS showed higher values in UTS for the +45°/-45° raster angle, and for strain at break +45°/-45° raster angle was predominant with a 117.25%. Interest feature showed for the polymeric blend of 75% SEBS-ABS is that +45°/-45° raster angle had the higher UTS amongst all of the raster angles used for the test. However, for the tensile strain the raster angle with the highest strain is the faux vertical, this value was not that greater than the one presented for the +45°/-45° raster angle, it was 5% smaller. In the case of 90%SEBS-ABS, values UTS and strain at break were predominant for raster angle +45°/-45°. Finally, for the 100% ABS polymeric blend values were higher for the raster angle of 0°/90° with no that much of difference in raster angle of +45°/-45°. Overall, values with the higher values in UTS and strain were presented in raster angles of +45°/-45° and 0°/90°.

5.1.5 Polymeric blends extruded with a single-screw extrusion system

The purpose of the following section will be to compare mechanical testing results of polymeric blends extruded in the single-screw extrusion system. Filaments with composition of 25%, 50%, 75%, and 90% SEBS-ABS were favored by using a raster orientation of +45°/-45°. Values obtained for UTS and strain at break were higher. Followed with the use of 0°/90° raster angle with a minimum difference amongst values. During the use of this extrusion system the trend was not the same in the case of polymer blend containing 100% ABS-MG94 for some reason the results were very close to each other but the predominance was for the faux vertical, followed up with the 0° /90° and +45° /-45° respectively. Overall, as indicated in sections 5.1.1 and 5.1.2, values for the use of the twin-screw extruder were higher than the ones with the use of the single-screw extruder. However, with regards of raster patterns used in each separate extrusion system, it seems that for both the +45° /-45° provided higher values for both, UTS and strain at break followed up with 0°/90°.

Table 5.2. Tensile test results from monofilaments extruded on the single-screw extruder along with their respective printed raster orientation.

MATERIAL	MODULUS YOUNGS (MPa)	ULTIMATE STRESS (MPa)	TENSILE STRAIN AT BREAK
	Average (Filabot)	Average(Filabot)	Average (Filabot)
25%SEBS-ABS			
+45°/-45°	1324.18 ± 113.33	21.19 ± 0.65	20.66 ± 6.33
0°/90°	1639.97 ± 314.70	19.32 ± 0.58	4.39 ± 2.32
90°	1031.98 ± 186.63	15.05 ± 1.65	5.16 ± 1.16
50%SEBS-ABS			
+45°/-45°	678.87 ± 37.29	14.07 ± 0.59	56.16 ± 11.43
0°/90°	844.09 ± 58.09	14.22 ± 1.05	45.38 ± 12.41
90°	348.04 ± 30.29	9.07 ± 0.93	15.31 ± 4.38
75%SEBS-ABS			
+45°/-45°	465.16 ± 33.86	10.35 ± 0.42	168.07 ± 34.73
0°/90°	608.68 ± 136.26	10.08 ± 0.49	81.62 ± 8.73
90°	146.37 ± 24.20	6.82 ± 0.52	118.67 ± 6.39
90%SEBS-ABS			
+45°/-45°	145.38 ± 39.00	10.78 ± 1.24	1262.59 ± 67.52
0°/90°	311.41 ± 114.69	10.37 ± 0.98	1033.73 ± 193.31
90°	38.78 ± 4.54	8.15 ± 0.48	836.14 ± 106.89
100%ABS			
+45°/-45°	2717.29 ± 210.91	33.90 ± 4.21	6.67 ± 4.81
0°/90°	2373.43 ± 306.37	33.92 ± 2.0	8.98 ± 2.19
90°	2187.56 ± 637.23	35.98 ± 1.51	9.00 ± 1.14

5.2 Rheological Results

Rheological results were obtained through the use of a melt flow indexer as previously mentioned. The results listed in table 5.3 showed a comparison between all of the polymeric blends with their respective extrusion systems. Results for 100% ABS-MG94 and 25%SEBS-ABS are close to each other by the use of two extrusion systems, a slight difference of 0.71g/10min and 0.2 g/10min respectively was registered. It is notable that the trend was not followed for the rest of the polymeric blends. Starting with 50% SEBS-ABS the twin-screw extruder showed a greater weight

(g/10min) than the weight obtained by the use of a single-screw extruder, difference in weight in between both values was of 12.11 g/10min.

Table 5.3. Melt Flow Index Results

Material	Filabot g/10min	Collin g/10min
ABS MG94	14.04	14.75
25 SEBS-ABS	19.5	19.7
50 SEBS-ABS	17.78	29.89
75 SEBS-ABS	20.65	16.38
90 SEBS-ABS	16.86	13.86

The opposite trend was encountered with the polymeric blend composed of 75% SEBS-ABS, the greatest amount was for the single-screw compared with the twin-screw extruder. Using the single-screw extruder 20.65g/10min was recorded as for the twin-screw extruder 16.38g/10min making a difference of 4.7g/10min. Finally, for the 90% SEBS-ABS blend the results were dominated by the use of the single screw extruder with a 16.86g/10min compared to 13.86g/10min in the twin-screw extruder. If the results are observed separately within each extrusion system, the single-screw extruder showed an increase in values when the percentage by weight of SEBS increased, when it reached to 50%SEBS-ABS there was a little decrease in weight and then increased again and decrease on the final blend (90%SEBS-ABS). This features support the mechanical test results, indicating that the performance of each extrusion systems behaves differently for flexible materials.

On the other hand, for the twin-screw extruder, values increased with the addition of SEBS in the polymeric matrix as well, the highest value was for the 50% SEBS-ABS with a 29.89g/10min. It was not the same case for the blends of 75% SEBS-ABS and 90%SEBS-ABS,

values decreased to 13g/10min. Overall, values were not close between the two extrusion systems within the incorporation of SEBS into the blends. Once the addition starts increasing values start to differ in a dissimilar manner. Based on this it can be observed that each system of extrusion behaves different within the addition of SEBS.

Based on a rheological study [45], theoretical values can be obtained by using Fox's law-type of equation and Law of averages-type approach, with the purpose to compare values reported by the melt flow index. Fox's law was used to calculate the glass transition temperature (Tg) of a blend is represented by the equation [49]:

$$\frac{1}{T_{gBlend}} = \frac{X_1}{T_{g1}} + \frac{X_2}{T_{g2}} \qquad (1)$$

X1 and X2 represent the weight fraction of each individual polymer. It is conceivable that the melt flow index of the blend can be calculated based the well-known Fox's law:

$$\frac{1}{MFI_{Blend}} = \frac{X_1}{\mathrm{MFI}_1} + \frac{X_2}{\mathrm{MFI}_2} \qquad (2)$$

In addition, a law of averages-type can be solved to predict the MFI of the binary blend by:

$$\mathrm{MFI}_{\mathrm{Blend}} = x_1\mathrm{MFI}_1 + x_2\mathrm{MFI}_2 \qquad (3)$$

In order to solve for the equations above, the melt flow index from baseline ABS-MG94 and SEBS were obtained. Values theoretically calculated by the use of the well-known Fox's law and law of averages-type formulas are reported in Tables 5.4 and 5.5.

Table 5.4. Melt Flow Index actual and theoretical results from filaments extruded in the twin-screw extruder.

Material	Collin g/10min	Fox's law-type calculation	Law of averages-type calculation
SEBS-g-MA	15.68		
ABS MG-94	14.75		
25 SEBS-ABS	19.70	14.98	14.98
50 SEBS-ABS	29.89	15.17	15.22
75 SEBS-ABS	16.38	15.40	15.44
90 SEBS-ABS	13.86	15.68	15.60

Interpreting the results in Table 5.4, it can be observed that the value of the lowest percent by weight that was incorporated into the matrix (25%SEBS-ABS), is greater than the baseline values reported by the melt flow index. In addition, the actual value is greater than the two theoretical values calculated. The highest value obtained for all of the polymeric blends was the one for the 50% by weight SEBS, with a 29.89g/10min; comparing the actual value to the theoretical, it is higher by 14.69g/10min (averaging both of the theoretical values calculated). In the case of 75% SEBS-ABS blend values from the MFI were very close to the ones calculated, with a difference of 0.96 g/10min. Finally, for the polymeric blend containing 90% by weight SEBS, there was a slight difference of 1.79g/10min. All of the polymeric blends with the exception of 90:10 blend ratio of SEBS and ABS were higher than the baseline values and theoretical, this indicates that rheological characteristics of the material is subjected to greater degree of SEBS [45].

Table 5.5. Melt Flow Index actual and theoretical results from filaments extruded in the single-screw extruder

Material	Filabot g/10min	Fox's law-type calculation	Law of averages-type calculation
SEBS-g-MA	15.68		
ABS MG-94	14.04		
25 SEBS-ABS	19.50	14.41	14.75
50 SEBS-ABS	17.78	14.79	14.86
75 SEBS-ABS	20.65	15.19	15.27
90 SEBS-ABS	16.86	15.50	15.51

Results obtained from blends extruded in the single-screw extruder, showed similar pattern compared to the ones discussed from the twin-screw extruder. Actual MFI values started to increase with the incorporation of SEBS in the polymeric matrix. MFI values from blends containing 25% and 50% by weight SEBS were higher than baseline and theoretical values. The blend with higher deviation from values calculated was for 75% by weight SEBS, with an actual value of 20.65 g/10min. On the other hand, 90% SEBS-ABS blend had a decrease of MFI value compared to the 75% SEBS-ABS. However, the respective value of 16.86g/10min was slightly higher than the values calculated.

Overall, theoretical values were calculated for comparison purposes with values reported by the MFI instrument. In addition, it allowed to observe whether the blends showed characteristics of alloying or blending. Values from both systems of extrusion did not deviate drastically from calculated and baseline values, with the exception of 50% SEBS-ABS from the filament extruded in the twin-screw extruder and 75% SEBS-ABS filament extruded in the single-screw extruder. For the rest of the filaments it can be concluded that polymer blending occurred. According to literature [45] polymer alloying can be possible in certain polymer mixture rations due to high

deviations from theoretical values, which could be the case for blends: (1) 50%SEBS-ABS extruded in twin-screw extruder and (2) 75%SEBS-ABS extruded in single-screw extruder.

5.3 Filament Tolerances

The diameter is an important parameter to take into account. Printing issues can arise if the filament does not meet the required size to feed the printer nozzle. Five measurements were taken from a length of 50cm for each of the filaments, this aided to monitor the precision of diameter size in both extrusion processes; as mentioned before the spooler instrument was the same for both process of extrusion. Values in Table 5.6: represent the diameter for each polymeric filament extruded by the single-screw and twin-screw extruders.

Table 5.6. Averages of the five diameter measurements that were taken for a length of 50cm of each of the filaments extruded in the single-screw extruder and twin-screw extruder

Material	Filabot diameter (mm)	Collin diameter (mm)
ABS MG94	1.69 ± 0.02	1.71 ± 0.02
25 SEBS-ABS	1.67 ± 0.02	1.70 ± 0.03
50 SEBS-ABS	1.68 ± 0.02	1.71 ± 0.02
75 SEBS-ABS	1.68 ± 0.02	1.72 ± 0.02
90 SEBS-ABS	1.69 ± 0.02	1.70 ± 0.01

The diameter values denoted in Table 5.6 indicates that the diameter for all of the filaments ranges from 1.67 to 1.72mm. These values were able to fit into the head of the printer, since the standard diameter size is 1.75mm. Diameters measured by the filaments extruded in single-screw extruder were slightly lower than the ones extruder in the twin-screw extruder. This was because the single-screw extruder has a fixed velocity compared to the twin-screw extruder. Overall, the diameters were within the size range, which is between 1.65mm-1.75mm.

5.4 Fractography

Fracture surfaces were analyzed and compared from samples printed and tested. The analysis was divided into three different categories according with the raster angle used: 45°, 0° and 90° with their respective extrusion system. The samples selected for the study were all the ones where the breakage occurred in the gage section. The use of a scanning electron microscope (SEM) was fundamental for this analysis.

According to literature, there exists different fracture characteristics that differ depending on the class of polymer that is used. For instance, a ductile mechanism is mostly present in thermoplastics due to the arrangements and stretching of thread-like macromolecules causing high deformation on the material. On the other hand, thermosets have a high level of cross-linkage in between polymer chains that do not present a high deformation as in the case of thermoplastics. In the case of elastomers, they present a small deformation in the material due to the elasticity characteristic that they possess [50].

5.4.1 Comparison of Fracture Surface of +45°/45° raster angle between single-screw and twin-screw extrusion system

The fracture surfaces of samples printed in the XYZ directions from baseline ABS-MG94 is represented in Figure 5.13. Observing the comparison of two processes of extrusion it can be noticeable that they both show a brittle behavior. In figure 5.13 (b) it can be seen the crack propagation from right hand corner up as represented with the arrows. In addition, there are some voids in the fracture surface; as it was mentioned before it is common that they appear between the print raster on material extrusion 3D printing.

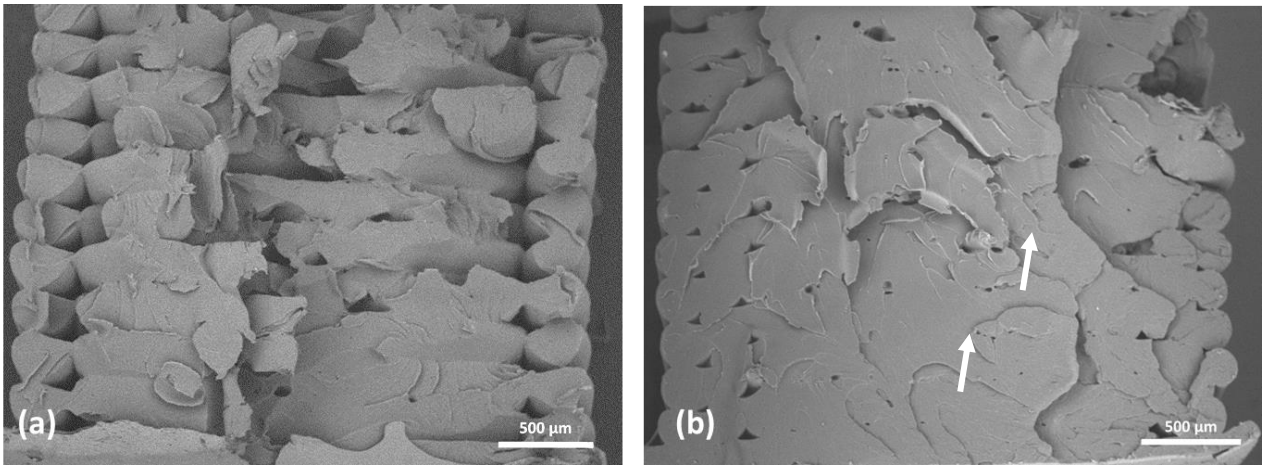

Figure 5.13.- Comparison of fracture surfaces of +45°/-45° raster angle: (a) 100% ABS-MG94 Collin (b)100% ABS-MG94 Filabot

Polymeric blends were rubberized by the increasing the percent by weight of the elastomer in the polymer matrix. Blends containing an amount of SEBS in the matrix presented a ductile mechanism. In other words, plastic deformation increased with the addition of SEBS (Figure 5.14 and Figure 5.15). Observing the effect of using both systems of extrusion, fracture surfaces look very similar for the exception of the blend containing 90% by weight SEBS. The sample which material was extruded using a twin-screw extruder, (Figure 5.15(c)) shows a slight plastic deformation compared to Figure 5.15(d), which is the sample printed using the filament extruded in the single-screw extruder (Filabot). This could be an indication of how different the extruders behave when the addition of SEBS by percent weight increases. Recalling on what was mentioned at the beginning of this section, elastomers show a very small plastic deformation which is what the sample in Figure 5.15(c) presents in the fracture surface. In other words, fracture surface in Figure 5.15(c) represents a brittle fracture compared to Figure 5.15(d). On the other hand, the fracture surface in Figure 5.15(d) represents a ductile fracture mode. This can indicate that the compounding was not the same when using a single-screw extruder for the blend 90%SEBS-ABS.

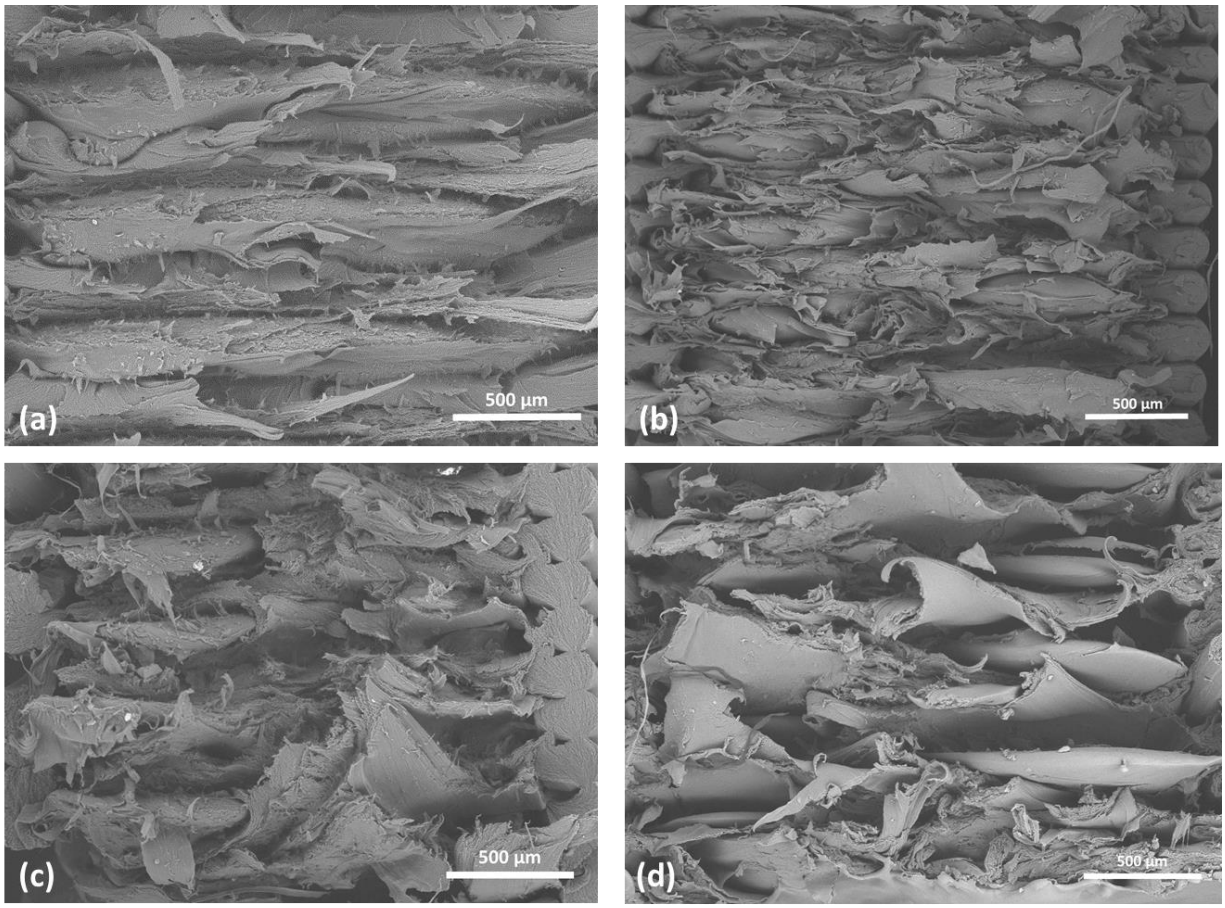

Figure 5.14.- Comparison of fracture surfaces of +45°/-45° raster angle : (a) 25% SEBS-ABS Collin; (b) 25% SEBS-ABS Filabot; (c) 50% SEBS-ABS Collin; (d) 50% SEBS-ABS Filabot

Fracture surface analysis can be correlated with the mechanical results presented, as the addition of the SEBS was made into the polymer matrix the UTS showed a significant decrease for the single-screw extruder. The same pattern was reported for the percent elongation or strain percent at break. This information can be relevant to understand the reason of the difference in fracture surface of the sample printed with the filament 90% SEBS-ABS. Both, the UTS and percent elongation values were lower for specimens printed with the filament that was produced by the single-screw extruder. This can indicate that the compounding in the single-screw extruder is not robust for blends with high percentage of SEBS.

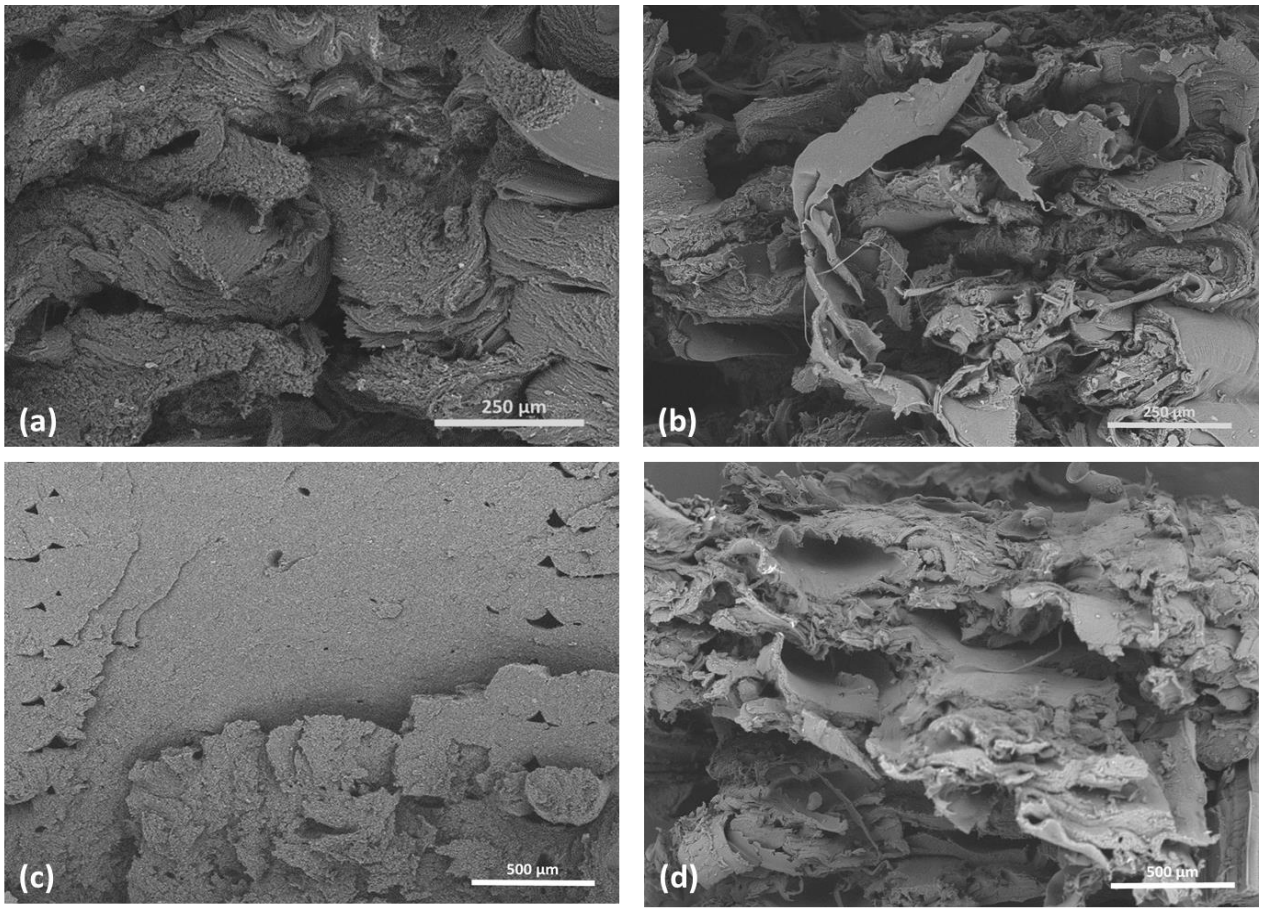

Figure 5.15.- Comparison of fracture surfaces of +45°/-45° raster angle : (a) 75% SEBS-ABS Collin; (b) 75% SEBS-ABS Filabot; (c) 90% SEBS-ABS Collin; (d) 90% SEBS-ABS Filabot

5.4.2 Comparison of Fracture Surface of 0°/90° raster angle between single-screw and twin-screw extrusion system

Fracture surface for specimens printed with a 0°/90° raster angle on a XYZ direction, showed similar features as the specimens presented for the +45°/-45° raster angle. Baseline (ABS-MG94) fracture surface is represented in Figure 5.10; it can be observed that fractures in both extrusion systems are brittle fractures. Due to print raster interface, fracture surfaces in Figures 5.16(a) and (b) show initiation of sites for craze indicated with the white arrows [45]. There is an evidence of the increase of plastic deformation correlated with the increase of SEBS in the polymer blends similar to the one presented in the +45°/-45° raster angle (Figure 5.11 and 5.12).

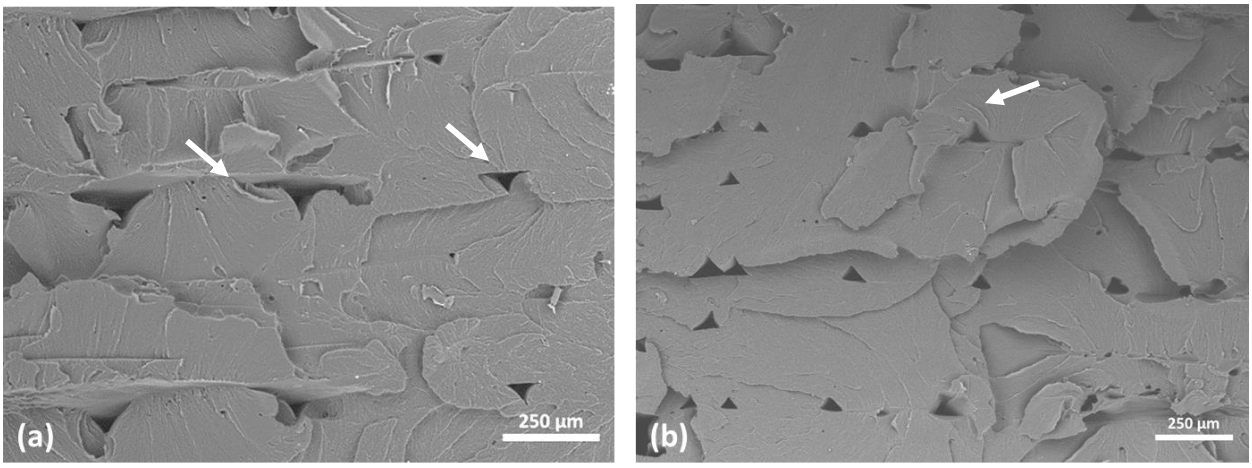

Figure 5.16.- Comparison of fracture surfaces of 0°/90° raster angle: (a) 100% ABS-MG94 Collin (b)100% ABS-MG94 Filabot

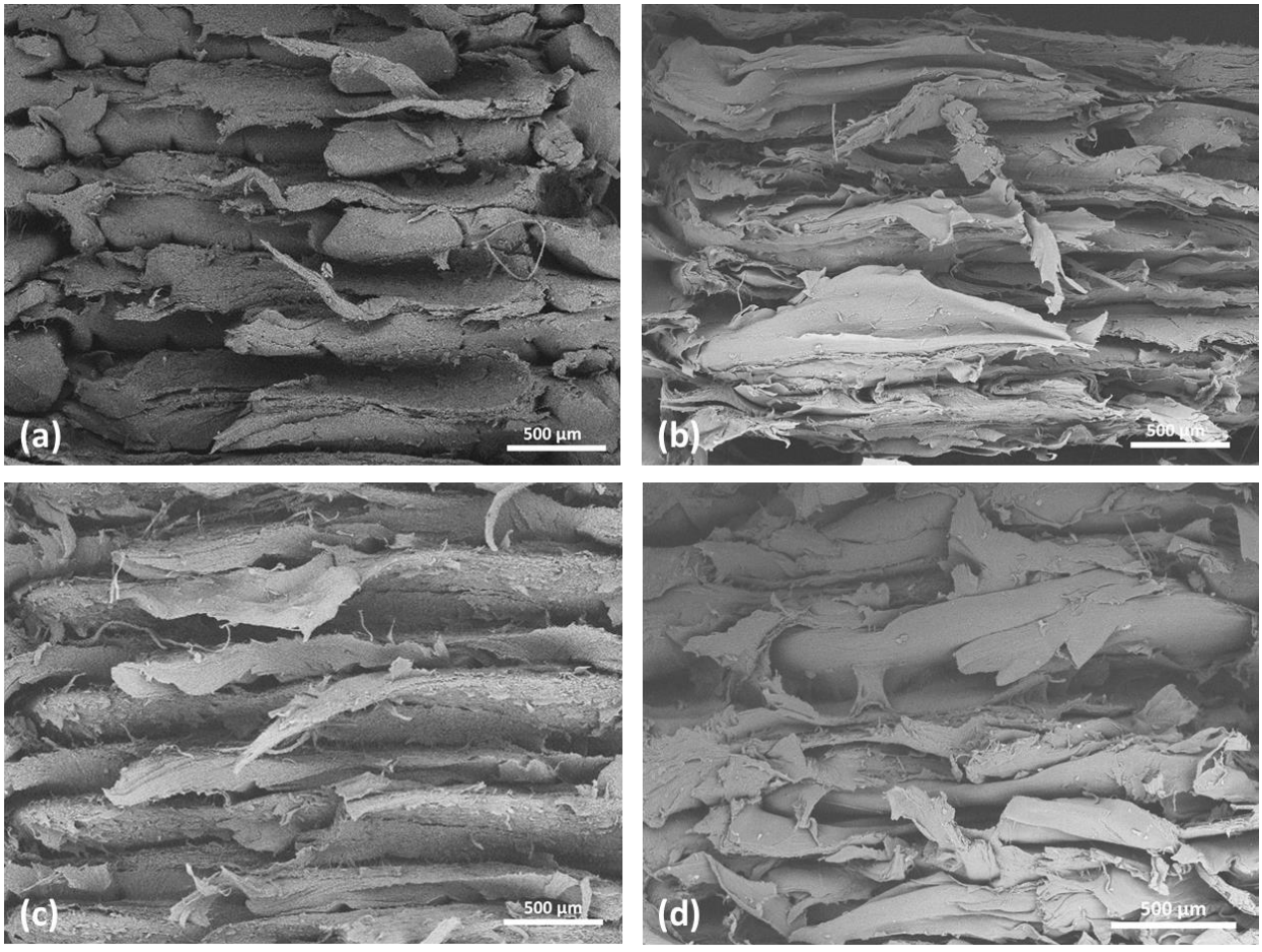

Figure 5.17.- Comparison of fracture surfaces of 0°/90° raster angle : (a) 25% SEBS-ABS Collin; (b) 25% SEBS-ABS Filabot; (c) 50% SEBS-ABS Collin; (d) 50% SEBS-ABS Filabot

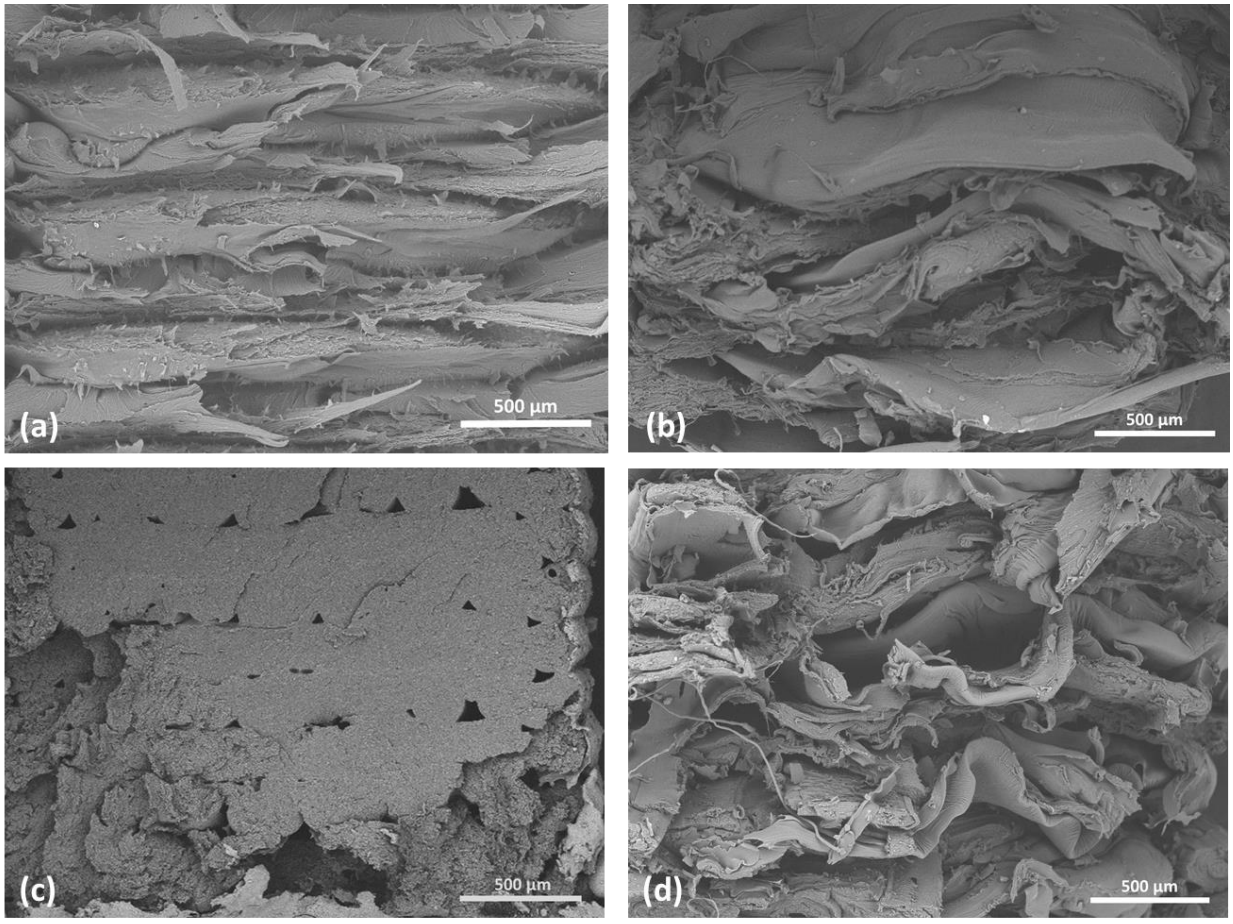

Figure 5.18.- Comparison of fracture surfaces of 0°/90° raster angle : (a) 75% SEBS-ABS Collin; (b) 75% SEBS-ABS Filabot; (c) 90% SEBS-ABS Collin; (d) 90% SEBS-ABS Filabot

Comparing the two systems of extrusion, the fracture surfaces look very similar to each other with the exception of 75% and 90% by weight SEBS. Observing at Figure 5.18 (a) and (b), it can be noticeable that there higher plastic deformation in the sample printed with filament produced from the single-screw extruder. However, there are not contingent with the results from the mechanical testing. The percent elongation is much higher in the specimen printed, from the filament produced with the twin-screw extruder than the one with the single-screw extruder. It is the same case for the blend containing 90% by weight SEBS Figure 5.18 (c) represents a brittle fracture mode compared to the Figure 5.12 (d), when in the mechanical test results the percent

elongation is greater for the filament extruded with twin-screw extruder compared to the single-screw extruder. The explanation of this feature could be that the blend contains mostly SEBS so it will have a high elongation causing a reduction in the cross-sectional area of the specimen. In addition, the elongation presented caused strain hardening effect on the polymer leading to a brittle fracture mode [45].

5.4.3 Comparison of Fracture Surface of 90° (faux vertical) raster angle between single-screw and twin-screw extrusion system

The fracture surface for baseline (ABS-MG94) specimens with a faux vertical raster are represented in Figure 5.19. Compared to the fracture surfaces previously analyzed for raster angles of 0° and 45° are similar with respect of the fracture mode, it is a brittle fracture mode. On the other hand, a different feature was found on the fracture surface that was not present in previous raster angles. Both systems of extrusions showed a cleavage stop, which commonly occurs in brittle factures [51]. This cleavage stop indicates the direction of propagation in the fracture surface from the two samples, represented in Figures 5.19 (a) and (b) with white arrows.

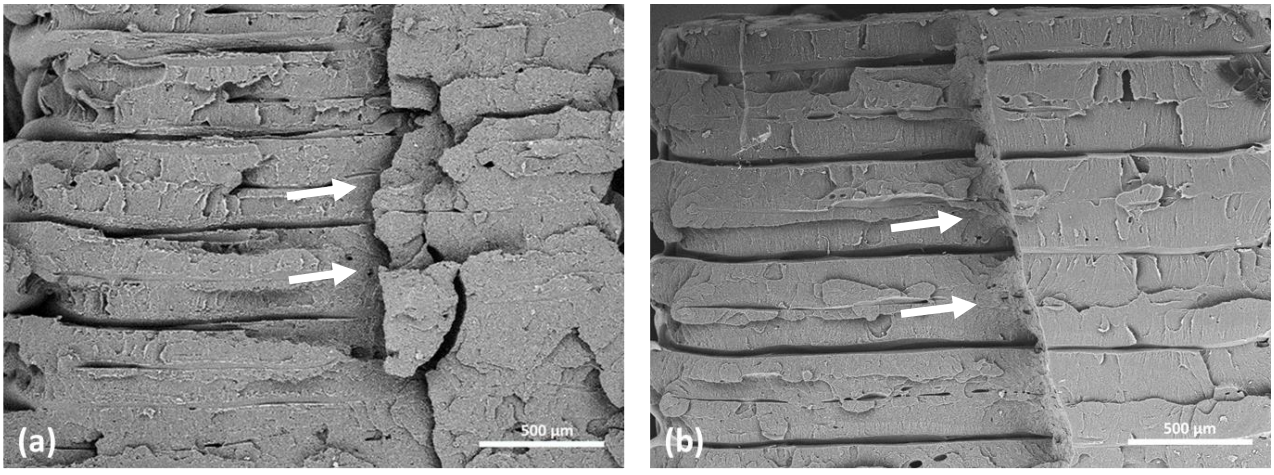

Figure 5.19.- Comparison of fracture surfaces of 90° (faux vertical) raster angle: (a) 100% ABS-MG94 Collin (b)100% ABS-MG94 Filabot

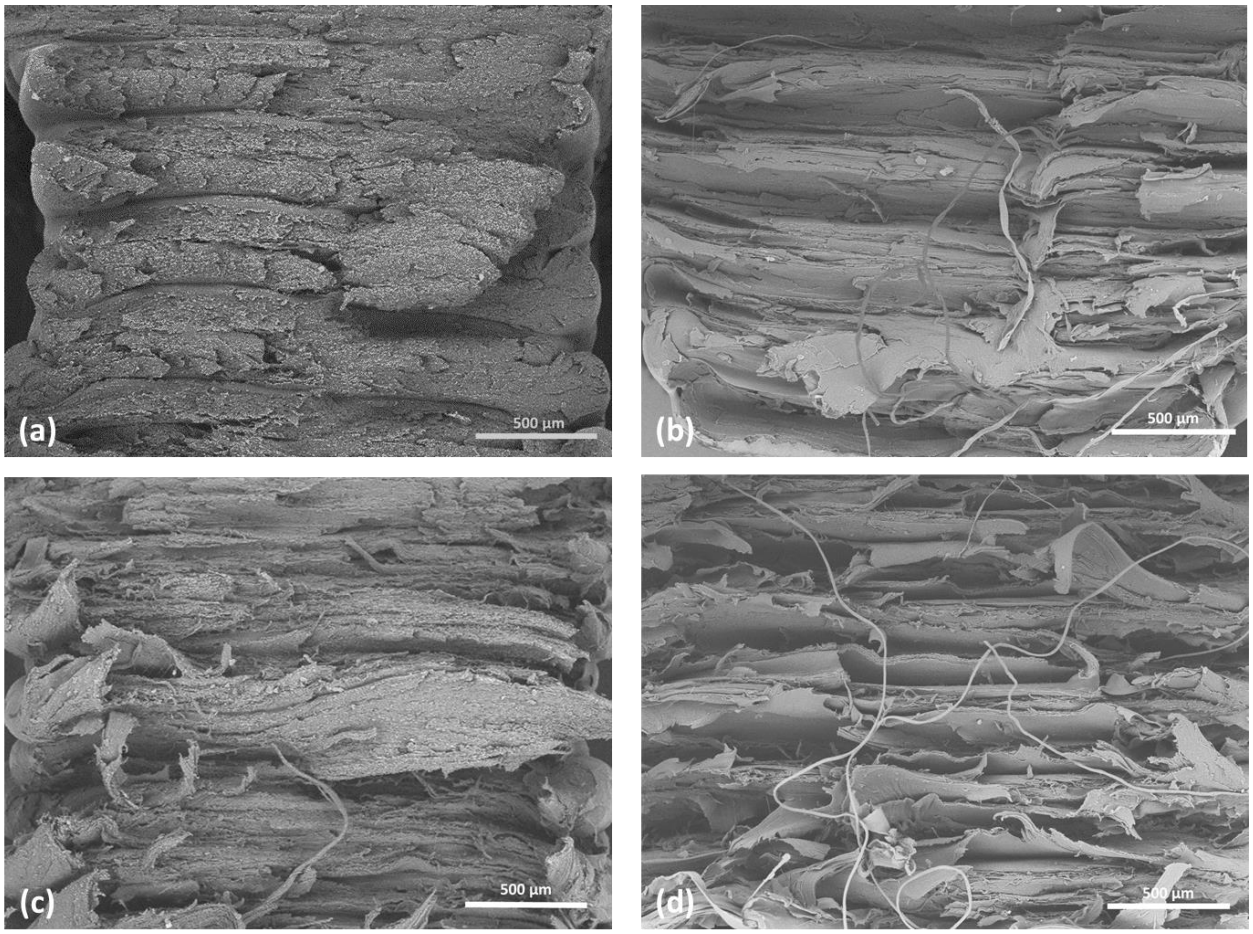

Figure 5.20.- Comparison of fracture surfaces of 90°(faux vertical) raster angle : (a) 25% SEBS-ABS Collin; (b) 25% SEBS-ABS Filabot; (c) 50% SEBS-ABS Collin; (d) 50% SEBS-ABS Filabot

Plastic deformation increased within the addition of SEBS into the polymeric matrix, which was previously observed with the rest of the raster patterns. Ductile fracture surfaces are represented in Figures 5.14 and 5.15. According to literature, a raster angle of 90° can be consider to be transversal which tends to have multiple fracture planes [48]. Figures 5.14 (a) and (b) showed a multiple fracture planes in the middle part of the specimens. Where Figures 5.14 (b) and (d) showed the presence of fibrils during the breakage of the sample. Fibrils usually indicate the stretch of carbon bonds in the system, due to the loading source that is been applied to break the tensile specimen. The highest plastic deformation was shown in Figure 5.15 since is all the samples are the ones with the higher percentage by weight of SEBS.

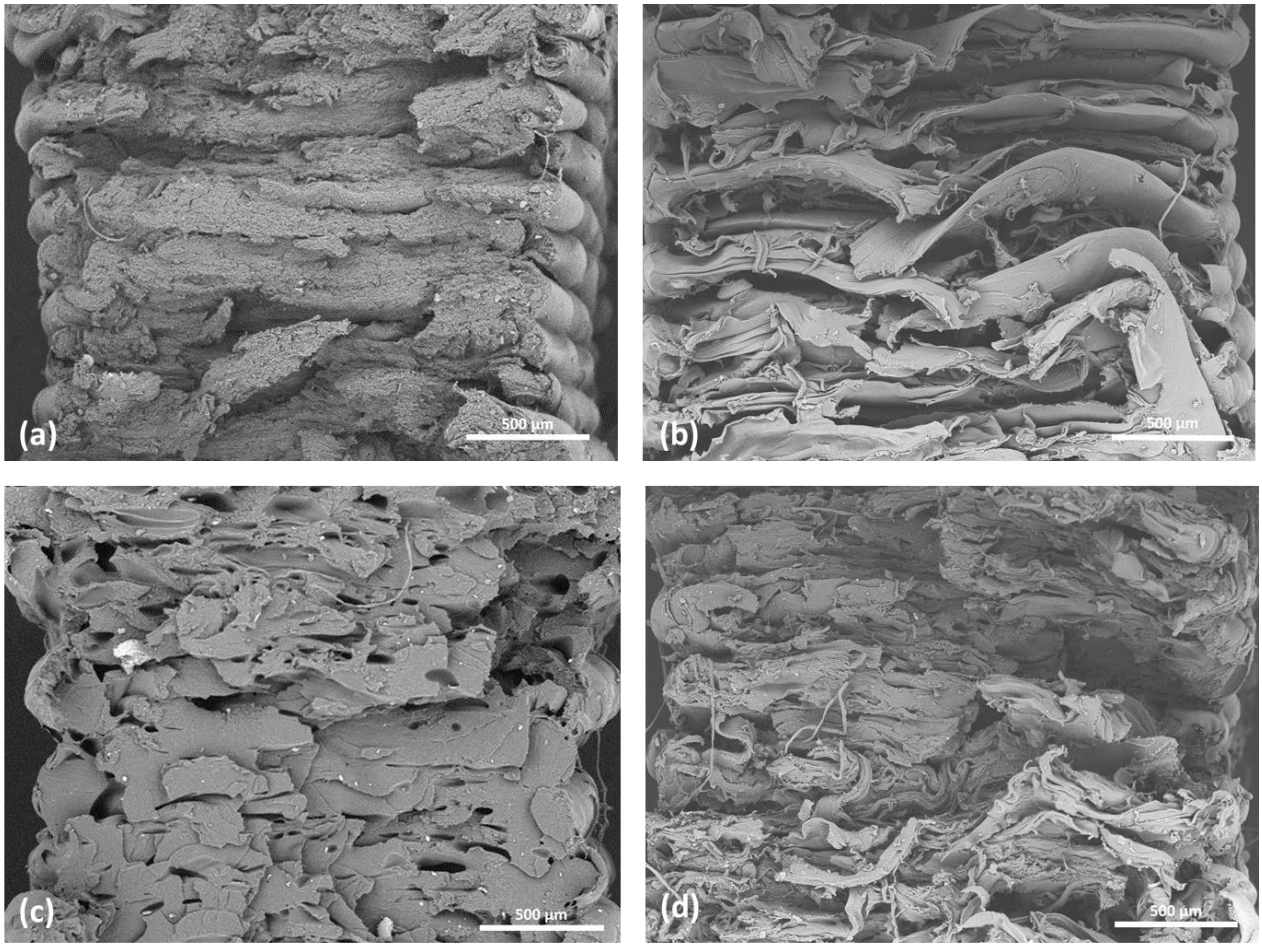

Figure 5.21.- Comparison of fracture surfaces of 90° raster angle : (a) 75% SEBS-ABS Collin; (b) 75% SEBS-ABS Filabot; (c) 90% SEBS-ABS Collin; (d) 90% SEBS-ABS Filabot

Figure 5.21(a) shows less plastic deformation than Figure 5.21(b), when the percent of elongation of specimens printed with filaments extruded from Collin was greater with 823.60% than in the Filabot 118.67%. The same feature is observed with specimens containing 90% by weight SEBS, plastic deformation is greater in specimens printed with filaments extruded with the Filabot than the Collin. This is similar to previous raster angles leading into the conclusion that brittle fracture is present in blends composed of 90%SEBS-ABS due to reduction of cross-sectional area of the specimen and strain hardening. Unfortunately, this did not occurred for filaments produced by the single-screw extruder leading the idea that the performance in compounding in the single-screw extruder is different than the twin-screw extruder [45].

Chapter 6: Conclusions

The aim of this study was to compare two extruder systems for 3D printer filament fabrication, to lead researchers a reference for the selection of their equipment. The two extruder systems that were compared consisted of: 1) a desktop grade single-screw extruder; and 2) an industrial grade twin-screw extruder. Differences between their performance and quality of mixing were studied by the extrusion of a rubberized blend of acrylonitrile butadiene styrene (ABS) mixed with styrene ethylene butylene styrene (SEBS). Different ratios were compounded in each extrusion system. Filaments were used to 3D print tensile specimens with raster angles of 45° 90° and 0°, to perform and compare mechanical testing. A rheological test was performed in filaments extruded in both systems of extrusion. Tolerances of filaments was important in order to record their diameters and deviations from the standard diameter required to feed the head of the printer. Finally, fracture surface was evaluated for all of the broken specimens to analyze differences of fracture modes between the extrusion systems and the difference in raster angles.

Mechanical results allowed to analyze the performance from both extrusion systems and differences in values between raster angles. The ultimate tensile strength (UTS) and percent elongation (%El) results from the twin-screw extruder predominated compared to results acquired from the single-screw extruder. The greatest deviation amongst values were noticeable as the incorporation of SEBS-g-MA increased, mainly in 50%, 75% and 90% by weight. It can be concluded that the twin-screw extruder has higher performance than the single-screw extruder, for the fabrication of flexible materials containing high ratios of SEBS into ABS. In regards of raster angles for each system of extrusion, it was observed that values were higher for angles of +45°/-45° and 0°/90°. Faux vertical specimens that were tested, show results with lower values for UTS

and %El compared to the rest of the raster angles. Higher mechanical properties can be achieved by the use of 45° and 90° raster angles, when using rubberized materials for 3D printing.

The rheological tests allowed to understand characteristics of blending and alloying in the polymeric matrix with respect to all of the ratios extruded. Melt flow index values obtained for each process of extrusion, were very similar for blends: 100% ABS-MG94 and 25% SEBS-ABS. However, they varied when the addition of SEBS was increased to an amount greater than 25%. This is an indication that the extruders perform differently with respect to mixing rubberized materials. Theoretical values were calculated, there was not a big deviation in values except for blends: 50% SEBS-ABS twin-screw extruder and 75% SEBS-ABS in the single-screw extruder. The higher deviations for these two filaments is an indication of alloying instead of blending. On the other hand, the rest of the filaments were close to baseline values and theoretical values as well, this indicates the characteristic of blending.

Tolerances from the diameters of the polymer filaments extruded, was another analysis that was done for this study. As mentioned before, the tests consisted on the evaluation of the filament's diameter, with the purpose to observe the precision and quality of the filament. During the two process of extrusion it was easier to control the diameter in the twin-screw extruder, due to the fact that the system counts with velocity controllers that allow adjustments in order to achieve the standard diameter required by the 3D printer. In the case of the single-screw extruder, controlling the diameter is not as easy as the twin-screw extruder, the only velocity that can be fixed is the one present in the spooler. The diameter values indicated by the single-screw extruder were lower than the ones obtained by the twin-screw extruder. The standard deviation from each system of extrusion was small, which indicates that diameters were constant for extrusion system. In

addition, even though diameters in the single-screw extruder were lower that twin-screw extruder, they all were closer to the standard diameter which is (1.75mm).

Fractography analysis was achieved by the use of scanning electron microscope. Fracture surfaces of tensile specimens that were 3D printed and tested were evaluated. The specific section of interest was the point of failure of the specimen. For all of the raster patterns used for the study, plastic deformation was prominent in filaments with high of percentages by weight of SEBS. In the case of 100% ABS-MG94, the main failure feature encountered was a brittle fracture mode. Filaments containing 90% by weight SEBS, were the ones with the most differences in fracture surface characteristics when comparing the two extruder systems.

According on tensile data reported for this study, the percent elongation of all the 90% by weight SEBS was higher in both systems of extrusion; however greater values were obtained for filaments extruded on the twin-screw extruder. As mentioned before, based on the fracture mode trend that was shown in SEM images within the addition of SEBS, it could be predictable that higher the plastic deformation will be for the higher loading used for the study (90% wt. SEBS-ABS). However, for the twin-screw extruder all the specimens presented a brittle fracture, which is expected for flexible materials that undergo trough a significant amount of plastic deformation. Brittle fractures occurred in flexible materials due to higher percent of elongation, meaning that a reduction of cross-section area is occurring in the specimen creating an instant fracture.

It is notable that a brittle fracture mode did not occurred for specimens that were printed with filaments extruded in the single-screw extruder; plastic defamation was encountered instead. This could be another evidence that the behavior of two extruders is different with respect to the mixing when the amount of elastomer in the mixture is increased. Finally, fracture modes for faux vertical specimens containing 100% ABS-MG94 showed a feature that was not present in

specimens with raster angles of 45° and 90° with the same material. Even though they presented brittle fracture modes the specimens with a faux vertical raster showed a cleavage stop indicating the direction of fracture propagation on the surface.

Overall, comparison of the performance or single-screw extruder and twin-screw extruder was achieved by the different tests discussed throughout this chapter. As it was hypothesized at the beginning of this analysis the performances of twin-screw extruder is better compared to single-screw extruder in terms of mixing. Most of differences between both extrusion systems was observable due to the increase of percent by weight SEBS-g-MA. However, single-screw extruder can be used for the extrusion of single materials, since less differences were encountered with respect to baseline material and 25% SEBS-ABS.

References

[1] R. Singh and S. Singh, "Additive Manufacturing: An Overview," in *Reference Module in Materials Science and Materials Engineering*, Elsevier, 2017.

[2] J. R. Wagner Jr., E. M. Mount III, and H. F. Giles Jr., "51 - Monofilaments," in *Extrusion (Second Edition)*, Oxford: William Andrew Publishing, 2014, pp. 585–591.

[3] M. Vaezi, S. Chianrabutra, B. Mellor, and S. Yang, "Multiple material additive manufacturing – Part 1: a review," *Virtual Phys. Prototyp.*, vol. 8, no. 1, pp. 19–50, Mar. 2013.

[4] D. Espalin, J. Ramirez, F. Medina, and R. Wicker, "Multi-Material, Multi-Technology FDM System." [Online]. Available: https://sffsymposium.engr.utexas.edu/Manuscripts/2012/2012-63-Espalin.pdf. [Accessed: 08-Mar-2017].

[5] Y. Huang, M. C. Leu, J. Mazumder, and A. Donmez, "Additive Manufacturing: Current State, Future Potential, Gaps and Needs, and Recommendations," *J. Manuf. Sci. Eng.*, vol. 137, no. 1, pp. 014001-014001-10, Feb. 2015.

[6] C. M. Shemelya *et al.*, "Mechanical, Electromagnetic, and X-ray Shielding Characterization of a 3D Printable Tungsten-Polycarbonate Polymer Matrix Composite for Space-Based Applications," *J. Electron. Mater. Warrendale*, vol. 44, no. 8, pp. 2598–2607, Aug. 2015.

[7] C. R. Rocha, A. R. T. Perez, D. A. Roberson, C. M. Shemelya, E. MacDonald, and R. B. Wicker, "Novel ABS-based binary and ternary polymer blends for material extrusion 3D printing," *J. Mater. Res.*, vol. 29, no. 17, pp. 1859–1866, 2014.

[8] R. Singh, N. Singh, P. Bedi, and I. P. S. Ahuja, "Polymer Single-Screw Extrusion With Metal Powder Reinforcement," *Ref. Module Mater. Sci. Mater. Eng.*, 2016.

[9] S. Singhal, V. K. Lohar, and V. Arora, "Hot melt extrusion technique," 2011.

[10] C. Abeykoon *et al.*, "A new model based approach for the prediction and optimisation of thermal homogeneity in single screw extrusion," *Control Eng. Pract.*, vol. 19, no. 8, pp. 862–874, 2011.

[11] C. I. Chung, "Extrusion of polymers Theory and Practice," *Hanser Munich*, pp. 1–47, 2000.

[12] B. Chen, L. Zhu, F. Zhang, and Y. Qiu, "Chapter 31 - Process Development and Scale-Up: Twin-Screw Extrusion," in *Developing Solid Oral Dosage Forms (Second Edition)*, Boston: Academic Press, 2017, pp. 821–868.

[13] E. M. Mount III, "12 - Extrusion Processes," in *Applied Plastics Engineering Handbook (Second Edition)*, M. Kutz, Ed. William Andrew Publishing, 2017, pp. 217–264.

[14] J. R. Wagner Jr., E. M. Mount III, and H. F. Giles Jr., "3 - Single Screw Extruder: Equipment," in *Extrusion (Second Edition)*, Oxford: William Andrew Publishing, 2014, pp. 17–46.

[15] J. R. Wagner Jr., E. M. Mount III, and H. F. Giles Jr., "11 - Twin Screw Extruder Equipment," in *Extrusion (Second Edition)*, Oxford: William Andrew Publishing, 2014, pp. 125–148.

[16] J. F. Stevenson, "10 - Extrusion of Rubber and Plastics," in *Comprehensive Polymer Science and Supplements*, G. Allen and J. C. Bevington, Eds. Amsterdam: Pergamon, 1989, pp. 303–354.

[17] J. R. Wagner Jr., E. M. Mount III, and H. F. Giles Jr., "4 - Plastic Behavior in the Extruder," in *Extrusion (Second Edition)*, Oxford: William Andrew Publishing, 2014, pp. 47–70.

[18] J. R. Wanger Jr., “Monofilaments - Extrusion (Second Edition) - 51.” [Online]. Available: http://www.sciencedirect.com/science/article/pii/B978143773481200051X?np=y&npKey=5b689860fbb1bf8988b02d86945ace915a406489224bc56d81ffe9c5d158832a. [Accessed: 05-Mar-2017].
[19] S. Sunpreet, R. Seeram, and S. Rupinder, “Material issues in additive manufacturing: A review.”
[20] J. W. Stansbury and M. J. Idacavage, “3D printing with polymers: Challenges among expanding options and opportunities,” *Dent. Mater.*, vol. 32, no. 1, pp. 54–64, Jan. 2016.
[21] X. Wang, M. Jiang, Z. Zhou, J. Gou, and D. Hui, “3D printing of polymer matrix composites: A review and prospective,” *Compos. Part B Eng.*, vol. 110, pp. 442–458, Feb. 2017.
[22] E. Kroll and A. Dror, “Enhancing aerospace engineering students’ learning with 3D printing wind-tunnel models: Rapid,” *Rapid Prototyp. J.*, vol. 17, no. 5.
[23] S. V. Murphy and A. Atala, “3D bioprinting of tissues and organs,” *Nat. Biotechnol.*, vol. 32, pp. 773–785, 2014.
[24] O. A. Mohamed, S. H. Masood, and J. L. Bhowmik, “Optimization of fused deposition modeling process parameters: a review of current research and future prospects,” *Adv. Manuf. Shanghai*, vol. 3, no. 1, pp. 42–53, Mar. 2015.
[25] I. Gibson, D. Rosen, and B. Stucker, *Additive Manufacturing Technologies*, Second. .
[26] I. Gibson, D. Rosen, and B. Stucker, “Development of Additive Manufacturing Technology,” in *Additive Manufacturing Technologies*, Springer New York, 2015, pp. 19–42.
[27] B. N. Turner, R. Strong, and S. A. Gold, “A review of melt extrusion additive manufacturing processes: I. Process design and modeling,” *Rapid Prototyp. J. Bradf.*, vol. 20, no. 3, pp. 192–204, 2014.
[28] B. C. Gross, J. L. Erkal, S. Y. Lockwood, C. Chen, and D. M. Spence, “Evaluation of 3D Printing and Its Potential Impact on Biotechnology and the Chemical Sciences,” *Anal. Chem.*, vol. 86, no. 7, pp. 3240–3253, Apr. 2014.
[29] T. Wang, J. Xi, and Y. Jin, “A model research for prototype warp deformation in the FDM process | SpringerLink,” *Int. J. Adv. Manuf. Technol.*, vol. 33, no. 11, pp. 1087–1096, Apr. 2006.
[30] K. G. Jaya Christiyan, U. Chandrasekhar, and K. Venkateswarlu, “A study of the influence of process parameters on the Mechanical Properties of 3D printed ABS composite,” *J. Mater. Eng.*, vol. 114.
[31] A. Kumar Sood, R. K. Ohdar, and S. S. Mahapatra, “Parametric appraisal of mechanical property of fused deposition modelling processed parts,” *Mater. Des.*, vol. 31, no. 1, pp. 287–295, Jun. 2009.
[32] O. S. Es-Said, J. Foyos, R. Noorani, M. Mendelson, R. Marloth, and B. A. Pregger, “Effect of Layer Orientation on Mechanical Properties of Rapid Prototyped Samples,” *Mater. Manuf. Process.*, vol. 15, no. 1, pp. 107–122, Apr. 2007.
[33] W. Wu, P. Geng, G. Li, D. Zhao, H. Zhang, and J. Zhao, “Influence of Layer Thickness and Raster Angle on the Mechanical Properties of 3D-Printed PEEK and a Comparative Mechanical Study between PEEK and ABS,” *Materials*, vol. 8, no. 9, pp. 5834–5846, Sep. 2015.

[34] T. Letcher, B. Rankouhi, and S. Javadpour, "Experimental Study of Mechanical Properties of Additively Manufactured ABS Plastic as a Function of Layer Parameters," *Addit. Manuf.*, vol. 2A, 2015.
[35] C. Comotti, D. Regazzoni, C. Rizzi, and A. Vitali, "Additive Manufacturing to Advance Functional Design: An Application in the Medical Field," *J. Comput. Infomation Sci. Eng.*, vol. 17, no. 3, 2016.
[36] S.-H. Ahn, M. Montero, D. Odell, S. Roundy, and P. K. Wright, "Anisotropic material properties of fused deposition modeling ABS," *Rapid Prototyp. J.*, vol. 8, no. 4, pp. 248–257.
[37] B. N. Turner and S. A. Gold, "A review of melt extrusion additive manufacturing processes: II. Materials, dimensional accuracy, and surface roughness," *Rapid Prototyp. J. Bradf.*, vol. 21, no. 3, pp. 261–250, 2015.
[38] M. Meryes and K. Chawla, *Mechanical Behavior of Materials*, Second. Cambridge University Press, 2009.
[39] M. F. Ashby and D. R. H. Jones, *Engineering Materials 2: Introduction to microstructures, Processing and Design*, Third. Elsevier, 2001.
[40] D. Whelan, "Chapter 24 - Thermoplastic Elastomers," in *Brydson's Plastics Materials (Eighth Edition)*, M. Gilbert, Ed. Butterworth-Heinemann, 2017, pp. 653–703.
[41] P. Spiridonov, E. Lambrinos, and Z. Peng, "Extrusion of monofilaments of thermoplastic elastomers," *Synth. Met.*, vol. 152, no. 1–3, pp. 61–64, 2005.
[42] "acrylonitrile-butadiene-styrene copolymer (ABS) | chemical compound," *Encyclopedia Britannica*. [Online]. Available: https://www.britannica.com/science/acrylonitrile-butadiene-styrene-copolymer. [Accessed: 27-Mar-2017].
[43] J. Rutkowski and B. Levin, "Acrylonitrile-Butadiene-Styrene Copolymers (ABS): Pyrolysis and Combustion Products and their Toxicity-A review fo the Literature," *Fire Mater.*, vol. 10, pp. 93–105, 1986.
[44] R. A. Shanks and I. Kong, "General Purpose Elastomers: Structure, Chemistry, Physics and Performance," in *Advances in Elastomers 1*, vol. 11, 2013, pp. 11–45.
[45] J. G. Siqueiros, K. Schnittker, and D. A. Roberson, "ABS-maleated SEBS blend as a 3D printable material," *Virtual Phys. Prototyp.*, vol. 11, no. 2, pp. 123–131, 2016.
[46] "ASTM D638-10. Standard test method for tensile properties of plastics," in *American Society for Testing and Materials*, West Conshohocken, PA: ASTM International, 2010.
[47] "ASTM D1238-13. Standard test method for melt flow rates of thermoplastics by extrusion plastometer," in *American Society for Testing and Materials*, West Conshohocken, PA: ASTM International, 2013.
[48] R. A. Torrado and A. D. Roberson, "Failure Analysis and Anisotropy Evaluation of 3D-Printed Tensile Test Specimens of Different Geometries and Pring Raster Patterns," *J Fail. Anal. and Preven.*, vol. 16, no. 1, pp. 154–164, Feb. 2016.
[49] W. Brostow, R. Chiu, I. M. Kalogeras, and A. Vassilikou-Dova, "Prediction of glass transition temperatures: Binary blends and copolymers," *Mater. Lett.*, vol. 62, pp. 17–18, Mar. 2008.
[50] A. R. T. Perez, D. A. Roberson, and R. B. Wicker, "Fracture surface analysis of 3D-printed tensile specimens of novel ABS-based materials," *J. Fail. Anal. Prev.*, vol. 14, no. 3, pp. 343–353, 2014.
[51] L. Engel, H. Klingele, G. Ehrenstein, and H. Schaper, *An Atlas of Polymer Damage-Surface examination by scanning electron mircoscope*. Wolfe Publishing Ltd.

Vita

Adriana Ramirez was born in El Paso TX, she was raised in Ciudad Juarez, Chihuahua, she moved to El Paso TX, in 2005 when she was in eighth grade. During her time in high school she became very interested in science, this motivated her to pursue a Bachelor's degree in Chemistry. In 2010, she decided to major in Chemistry at the University of Texas at El Paso. During her time pursuing her Bachelor's degree, she was selected to be an officer from the American Chemistry Society (ACS). During a year she motivated students from all grades to pursue a College degree. Two years later, she received an award by the Research Initiative for Scientific Enhancement (RISE).

This award allowed Adriana to perform research in Materials Research and Technology Institute at UTEP, under the direction of Dr. Russell Chianelli and supervision of Dr. Torres and Dr. Zarei. She acquired experience and skills in the area of Materials Science during the two years she worked at this laboratory. Adriana earned her Bachelor's degree in Chemistry in May 2014. Working in the area of Materials Science research encouraged her to pursue a Master's Degree in Materials Science Engineering at the University of Texas at El Paso. Adriana was given the opportunity to work in a Polymer Extrusion Lab under the direction of Dr. David A. Roberson, once she was accepted into her Master's program. Adriana was able to learn about a different research field, she acquired skills in Additive Manufacturing Technologies, as well as extrusion processes for the production of polymeric filaments used for 3D printing.

Contact Information: aramirez53@miners.utep.edu

This thesis was typed by Adriana Ramirez.